EPJ Web of Conferences **348,** 03005 (2026) https://doi.org/10.1051/epjconf/202634803005
ICMSI 2026

Photocatalytic Degradation of Various Dyes using Spinel Aluminates and Their Composites: A Review

Krunal D. Solanki[1,2], *Ashish* R. Tanna[1], and *Harshal* B. Desai[1]*

[1]Department of Physics, School of Science, RK University, Rajkot 360 020, Gujarat, India

[2]Goverment Arts, Commerce and Science College, Deodar 385330, Gujarat, India

Abstract. Toxic, cancer-causing and hazardous organic dyes are increasingly being released into the Earth's drinking water through large industries, humans, and various other sources. Removing these contaminants has become extremely essential. Although physical, chemical and biological methods are being used to eliminate such pollutants, they are often not completely effective. At present, Advanced Oxidation Processes (AOPs) are being widely adopted for better results. In our review paper, we discuss how spinel aluminate can be used as a catalyst for the degradation of such harmful organic dyes. Spinel aluminate oxides have garnered attention due to their multifunctional properties and broad applicability. These materials exhibit exceptional stability, tuneable band gaps, and strong surface activity, which make them suitable for catalysis, sensors, energy storage, and environmental remediation. Among these, photodegradation of organic pollutants from wastewater is one of the most promising applications. In comparison to conventional methods such as adsorption, filtration, and reverse osmosis, spinel aluminate oxide-based photocatalysis delivers notable advantages: low cost, reusability, and the ability to mineralize diverse hazardous contaminants into safe products. This review covers the types of spinel aluminates, their composites, synthesis methods, and photocatalytic performance against various dyes.

1. Introduction

In today's rapidly developing era, various industrial sectors are growing quickly, including the leather industry, textile industry, printing industry, and others. Due to such industries, toxic, carcinogenic, and hazardous organic dyes (e.g. Methylene Blue, Methyl Orange, Rhodamine B, Malachite Green, Crystal Violet, Congo Red, Reactive Black, Tetracycline, etc.) are released into the Earth's water. These substances are extremely dangerous for humans as well as for all living organisms. Moreover, the amount of potable water available on Earth is already very limited, and that too is becoming increasingly contaminated, which has become one of the major problems today. Removing organic dyes from water can be done using physical, chemical, or biological methods. Common approaches include membrane filtration, reverse osmosis, chemical precipitation, coagulation, adsorption, and

*Corresponding author: harshal.desai@rku.ac.in

© The Authors, published by EDP Sciences. This is an open access article distributed under the terms of the Creative Commons Attribution License 4.0 (https://creativecommons.org/licenses/by/4.0/).

biological treatment. [1-3]. Traditional methods often produce sludge or other secondary pollutants, requiring extra purification steps. To address these issues, advanced oxidation processes (AOPs) have become a promising solution. One standout approach is photocatalytic degradation with semiconductor catalysts, which can break down dyes and other organic pollutants into harmless substances like carbon dioxide and water, either partially or completely [4]. Spinel oxides have shown significant advancements in applications such as catalysis, sensors, batteries, dye degradation, and drug delivery. Recently, most research has focused on their photocatalytic activity, as the efficient removal of organic contaminants from wastewater is a major environmental concern. Compared to conventional methods like desalination, adsorption, and reverse osmosis, photocatalytic degradation offers a more effective and sustainable treatment approach.[5]. In today's time, many spinel oxides are being used as photocatalysts, and among them, aluminate-based photocatalysts are gaining wide application. Researchers are currently exploring how such spinels can deliver the best possible performance as photocatalysts and how they can be designed with an appropriate energy band gap. Considering the various properties and applications of spinel oxides, the general formula of spinel compounds is MB_2X_4, where M mainly represents +2 valence ions (such as Zn, Mg, Ba, Ca, Cu) and B mainly represents +3 valence ions (such as Cr, Ga, In, Fe, Al). X is generally oxygen or sulphur. Due to the diverse properties of such spinels, their importance in the research field has been increasing significantly today. [6-7]. They have summarized different synthesis methods of spinel oxides, including solid-phase, liquid-phase, and vapour-phase methods. They have reviewed that the versatile properties of spinel oxide are highly dependent on the cations at the tetrahedral sites(A) and octahedral sites (B), and the synthesis conditions. They have shown that their widespread applications are in magnetic and optical devices, gas sensing, energy storage, catalysis, and photocatalysis. provided information about the catalytic and photocatalytic properties of spinel oxides, and they showed that the catalytic activity of oxide spinels is heavily influenced by the distribution of cations between tetrahedral and octahedral sites [8].

2. Spinel Aluminate Oxides

Spinel aluminate oxides are inorganic compounds with the general formula AB_2O_4, where M is a divalent metal ion like Zn^{2+}, Co^{2+}, Ni^{2+}, Cu^{2+}, or Mg^{2+}. They crystallize in a cubic spinel structure (Fd3m), with M^{2+} ions in tetrahedral sites and Al^{3+} ions in octahedral sites, which gives them high thermal stability, chemical resistance, and strong mechanical strength. These oxides have an FCC-type structure and usually feature a wide band gap, making them great for photocatalytic uses like dye degradation [1].

2.1 Normal Spinel Aluminate Oxides

The divalent metal ion M^{2+} is situated at the tetrahedral site (A) and two Al^{3+} ions are situated at the octahedral site (B) in normal spinel Aluminate. The general formula of cation distribution of normal spinel Aluminate is (M) $A[Al_2]BO_4$. Examples of normal spinel Aluminate are Zinc Aluminate ($ZnAl_2O_4$) and Copper Aluminate ($CuAl_2O_4$). Here, Zn^{2+} and Cu^{2+} ions occupy the tetrahedral sites (A), while Al^{3+} ions are found at the octahedral sites (B). Normal spinel aluminate has several applications, including dye degradation, use as a fluorescent material, antimicrobial and biodegradable purposes, and photocatalysis [1-3].

2.2 Inverse Spinel Aluminate Oxides:

The divalent metal ion M^{2+} is situated at the octahedral site (B), one trivalent Al^{3+} ion is situated at the tetrahedral site (A) and one trivalent Al^{3+} ion is situated at the octahedral site (B) in inverse spinel Aluminate. The general formula of cation distribution of inverse Spinel Aluminate is (Al)A [M Al]BO_4. Examples of inverse spinel Aluminates are Nickel Aluminate ($NiAl_2O_4$), Aluminate ($FeAl_2O_4$). Can be used as photocatalysis, electrocatalysis (OER), sensors, magnetic materials, pigments and electrodes etc [1-3].

2.3 Mixed/Random Spinel Aluminate Oxides:

In random spinel aluminate, the divalent metal ions (A^{2+}) and trivalent aluminium ions (B^{3+}) are distributed across both the tetrahedral (A) and octahedral (B) sites. The general formula of cation distribution of inverse Spinel Aluminate is (M_{1-x} Al_x) A [M_x Al_{2-x}]BO_4. An example of inverse spinel aluminate is Nickel Aluminate ($NiAl_2O_4$), at high annealing temperatures (>1000 °C) or in nanocrystalline form, Ni^{2+} and Al^{3+} show random distribution between tetrahedral and octahedral sites. Cobalt Aluminate ($CoAl_2O_4$) There are various applications of Mixed/Random Spinel Aluminate Oxides like ceramic pigment, catalyst, photocatalytic activity etc [1-3].

3. Photocatalytic Dye Degradation:

To remove organic dyes, present in water, various types of photocatalysts are used, which break down the harmful dye molecules in wastewater under light irradiation. Semiconductor-based photocatalysts are commonly used because they have a band gap. When employed for photocatalytic dye degradation, exposure to suitable light excites generates electrons and holes due to the band gap. The oxidation and reduction reaction takes places in the solution due to electron- hole pair. As a result, form free radicals likes hydroxyl radicals and superoxide radicals, which attack the dye molecules and decompose them into harmless substances like carbon dioxide and water. This process is simple, cost-effective, and environmentally friendly, which makes it widely used [4].

4. Photocatalytic Applications of Spinel Aluminate:

Spinel aluminate works as a photocatalyst by using electromagnetic radiation to create electron–hole pairs on its surface. These pairs trigger oxidation and reduction reactions in the solution, producing reactive species like hydroxyl and superoxide radicals. These radicals play an important role in breaking down organic dyes. Moreover, when electrons and holes interact with surface-adsorbed H_2O or OH^-, more hydroxyl radicals are generated. These radicals are the main active agents behind the photocatalytic degradation of dyes [1]. The photocatalytic applications of different spinel aluminates are discussed in the next section.

4.1 Photocatalytic Application of Pristine Spinel Aluminate

Hakki Hamid Kazemi et al. developed $ZnO/ZnAl_2O_4$ spinels. They evaluated the material's photocatalytic performance for treating wastewater containing methylene blue (MB) using a modified sol-gel method. The Al-modified spinel achieved 93% degradation of MB at pH 9 within 90 minutes under visible light, significantly outperforming pure ZnO [9]. Javed Muhammad et al. synthesised $ZnAl_2O_4$ using a sol-gel auto combustion method. $ZnAl_2O_4$ works well for breaking down Crystal Violet (CV) under sunlight. It's been observed that the degradation percentage of CV goes up with longer light exposure, reaching an impressive 80% removal after 120 minutes [10]. They synthesised a ZnAl-layered double hydroxide (LDH) catalyst using the co-precipitation method and studied its photocatalytic degradation of Rhodamine B (RhB) under both UV and solar light. The resulting CZA4 material showed high photocatalytic efficiency, achieving approximately 100% discoloration of RhB in 90 minutes under both UV and solar radiation. [11]. Chaudhary Archana et al. synthesised $ZnAl_2O_4$ nanoparticles using a sol-gel route, focusing on a surfactant-mediated approach to obtain phase-pure particles and studying their photocatalytic degradation of various organic dyes. They concluded that the use of surfactants reduced the particle size of $ZnAl_2O_4$ nanoparticles from 12 nm to 6 nm. The catalyst prepared with the cationic surfactant (CTAB) exhibited a high surface area (129.62 m^2/g) and a positive surface charge, leading to better adsorption (up to 41%) and degradation (97–99%) efficiency for anionic dyes like Eosin B and Congo Red. The catalyst was also reusable for up to four cycles [12]. Putra Ageng Trisna et al. prepared zinc aluminate ($ZnAl_2O_4$) spinel from layered double hydroxide (LDH) precursors and investigated its photocatalytic activity for p-nitrophenol reduction. The initial LDH was prepared by a co-precipitation technique. They concluded that the LDH precursor successfully formed a mesoporous α-$ZnAl_2O_4$ spinel structure with a high BET surface area and an average crystallite size of 9.3 nm when heated at 700 °C. This material showed excellent photocatalytic performance, reducing p-nitrophenol in at least 9 minutes under visible light irradiation [13]. $ZnAl_2O_4$ spinel nanoceramics synthesised using a sol-gel combustion method and evaluated their photocatalytic activity for both H_2 production and methylene blue (MB) dye degradation. Annealing at temperatures between 500 °C and 900 °C produced crystalline spinels, with formation occurring at temperatures as low as 500 °C. The characteristics of the $ZnAl_2O_4$ spinels were strongly influenced by the annealing temperature. The sample treated at 500 °C achieved the best H_2 evolution, producing 145 μmol g^{-1} after 2 hours. In contrast, the sample treated at 900 °C showed the highest dye degradation, removing 84% of MB dye after 120 minutes of UV irradiation [14]. Han Mei et al. synthesised a series of aluminate spinels like, $MgAl_2O_4$, $CoAl_2O_4$, $NiAl_2O_4$, $CuAl_2O_4$, and $ZnAl_2O_4$) and investigated their physical properties, including magnetic and heat capacity characteristics.The spinels were synthesised using a solution combustion method with glycine as the fuel, followed by secondary calcination at temperatures between 900 °C and 1100 °C. The synthesis produced pure spinel phases with porous structures composed of nano-sized particles. The study detailed the magnetic properties, finding that $CoAl_2O_4$ and $CuAl_2O_4$ exhibited strong geometric magnetic frustration. The physical properties were found to be dependent on the A-site ions [15]. Battiston Suellen and colleagues synthesised $ZnAl_2O_4$ spinel and tested its use as a photocatalyst for breaking down tannery dye under sunlight. The $ZnAl_2O_4$ spinel was synthesised by co-precipitation method. The material showed promising photocatalytic activity, with degradation efficiency decreasing as the initial dye concentration increased. It successfully degraded Direct Black 38 dye under sunlight [16]. Wang Shi-Fa et al. were prepared three different $ZnAl_2O_4$ samples via a modified polyacrylamide gel method. The experimental results show the phase purity, particle size, morphology, and the optical and fluorescence properties of $ZnAl_2O_4$ nanoparticles. These kind properties of material also play crucial role in photodegradation of dyes [17]. Tangcharoen Thanit et al. synthesized $NiAl_2O_4$, $CuAl_2O_4$, and $ZnAl_2O_4$ aluminate spinel nanoparticles using a sol-gel auto-combustion method. The band gap energies of these nanoparticles influence their photocatalytic activity. Among them, $NiAl_2O_4$ and $CuAl_2O_4$ demonstrated higher photocatalytic performance than $ZnAl_2O_4$ due to their lower band gaps, achieving dye degradation efficiencies of 80–95% within 100 minutes under UV light. [18]. They have synthesised $MnAl_2O_4$-$ZnAl_2O_4$ nanomaterial using a co-precipitation method. They have concluded that the mixed-phase nanocomposite with a crystallite size of 48.5 nm. It exhibited excellent photocatalytic activity against Methyl Violet dye, (91% efficiency).

$MnAl_2O_4$-$ZnAl_2O_4$ nanomaterial also useful as an anti-bacterial activity. [19]. M. Serdechnova et al. produced composite coatings of ZnO and $ZnAl_2O_4$ on zinc substrates using Plasma Electrolytic Oxidation (PEO) in a phosphate-aluminate electrolyte. With the coatings improved wear and corrosion resistance, hence photocatalytic activity for degrading methyl orange (MO) is decreases, because the band gap has increased to more than 3.9 eV, it does not allow excitation in either the visible or A light range. The highest activity was observed for samples processed for 12 minutes at 100 and 125 mA/cm², which contained the highest amount of ZnO [20]. $ZnAl_2O_4$ nanoparticles were synthesised using a solution combustion method by Shilpa G. et al. The nanoparticles had an average crystallite size of 37 nm and a band gap of 3.07 eV. The photocatalyst showed excellent degradation of Acid Red 88 dye achieving a maximum of 98.44% under natural sunlight in 90 min. [21]. Salavati-Niasari et al. prepared nanocrystalline Copper Aluminate ($CuAl_2O_4$) through a modified Pechini sol-gel process.The precursor was heat-treated at 600 °C to form pure crystallized $CuAl_2O_4$ nanocrystals with a size of about 17–26 nm, and the use of citric acid was found to inhibit particle growth, reducing the average crystallite size from 28 nm to 17 nm. The material had a calculated band gap of 2.10 eV. [22]. Khalifeh Reza et al. synthesised $CuAl_2O_4$ nanoparticles using a programmable hydrothermal method. They have successfully demonstrated that the synthesised hollow spheres acted as efficient heterogeneous catalysts for the chemical fixation of CO_2. The flower-like triple-shelled $CuAl_2O_4$ made with a glucose template showed the highest catalytic performance, achieving up to a 98% isolated yield under optimised conditions. [23]. Hosseini S. Akbar. synthesised $CuAl_2O_4$ nanostructures using a sol-gel method and different amino acids as fuel and investigated their photocatalytic application for the degradation of methyl orange. The synthesis produced pure cubic phase $CuAl_2O_4$ nanostructures with an average particle size of 30–40 nm when using cysteine and asparagine. The material exhibited superparamagnetic behaviour and had a band gap of 3.07 eV. It showed high photocatalytic activity, degrading 90% of methyl orange in 80 minutes under UV light [24]. Dabhade Ganesh et al. synthesized nanocrystalline copper aluminate ($CuAl_2O_4$) and tested its photocatalytic activity for degrading indigo carmine (IC) dye under UV light. The $CuAl_2O_4$ was synthesised using a simple and economical solid-state mechanochemical (MCH) method. The material was highly effective, achieving 99% degradation of an 8 ppm IC dye solution in 25 minutes under UV radiation. The catalyst also showed remarkable reusability and stability over five consecutive cycles [25]. Kaci M. M. et al. synthesized $CuAl_2O_4$ nanoparticles using a nitrate route, which involved dissolving metal nitrates in HNO_3, then evaporating and calcining at 850 °C for 18 hours. They studied the material's performance in the photocatalytic degradation of Basic Red 46 (BR 46) dye under visible light. The resulting spinel had a crystallite size of 19 nm, a surface area of 44.22 m²/g, and an indirect bandgap of 1.80 eV. Under pH 10 conditions, the photocatalyst achieved 93% degradation of BR 46 within 120 minutes of visible light exposure and showed good stability and reusability over five cycles. [26]. Abed Sattar H. et al. synthesized $CuAl_2O_4$ nanoparticles using the co-precipitation method for the photocatalytic degradation of Methyl Violet dye under both UV and visible light. The resulting nanoparticles had a crystallite size of 19.57 nm and a direct band gap of 3.46 eV. The photocatalyst successfully degraded 72.49% of Methyl Violet within 120 minutes under these conditions. The material also demonstrated good stability and reusability over five cycles, maintaining over 68% efficiency [27]. Mosleh Mohammadreza, et al. synthesised nanocrystalline cobalt aluminate ($CoAl_2O_4$) through an auto-combustion method using amino acids like glycine as fuel, followed by calcination at 800 °C. The spherical nanoparticles, measuring 30–35 nm, were used to break down methyl orange (MO) under UV light, reaching 76% decolorization in 70 minutes. [28]. A mesoporous $CoAl_2O_4$ spinel were synthesised through a combustion method using triethanolamine as fuel, followed by thermal decomposition by Guo Sheng et al. The $CoAl_2O_4$ exhibited remarkable catalytic activity for degrading Rhodamine B (RhB) through peroxymonosulfate (PMS) activation. The photocatalyst broke down 99% of RhB in just 20 minutes, with a degradation rate 89 times faster than Co_3O_4 and 10.5 times faster than precipitation-prepared $CoAl_2O_4$. This impressive performance is due to its large surface area, mesoporous structure, and excellent electrical conductivity [29]. Blue spherical $CoAl_2O_4$ pigment powder synthesized and investigated the effects of pH and temperature on its properties. The pigment was synthesised by co-precipitation. They concluded that the spherical pigment powders with a core-shell structure and high purity. The colour and morphology were highly dependent on pH and hydrothermal temperature [30]. Gholami Tahereh et al. prepared $CoAl_2O_4$ pigments and investigated their photocatalytic and electrochemical hydrogen storage properties.The $CoAl_2O_4$ pigments were synthesised via a thermal decomposition method. The material showed photocatalytic activity, degrading 37% of methylene blue in 80 minutes under UV light. Additionally, it demonstrated a significant hydrogen storage capacity of 1100 mAh/g after 20 cycles in electrochemical tests [31]. Cobalt Aluminate ($CoAl_2O_4$) nanoparticles prepared using the Solution Combustion Method. The photocatalytic activity was tested on methylene blue dye. The sample annealed at 900 °C showed the best performance, with 64% degradation [32]. Fangli Yu et al. prepared nanosized cobalt aluminate ($CoAl_2O_4$) spinel powders using sol–gel and sol–gel hydrothermal methods. They found the sol-gel-hydrothermal method to be superior for preparing nanosized $CoAl_2O_4$ powders. While the conventional sol-gel method required a high temperature of 1000 °C and produced agglomerated particles of 100–200 nm, the combined sol-gel-hydrothermal process yielded pure, non-aggregated nanoparticles of 50–60 nm at a significantly lower temperature of 250 °C [33]. Boudiaf S. and colleagues synthesized the semiconductor $CoAl_2O_4$ using a chemical nitrate method, producing a single spinel phase with n-type conductivity and an optical band gap of 1.83 eV. A hetero-system of $CoAl_2O_4$/ZnO was used as a photocatalyst, which degraded 94% of Congo Red dye in 240 minutes under visible light irradiation [34]. Magnesium Aluminate Nanoparticles synthesized using the molten salt method. The material showed excellent thermal stability, with only a 3% weight loss at 600 °C, making it suitable for refractory crucible applications [35]. Mahi K. et al. Synthesised and characterised nanocrystalline magnesium and barium aluminates using sol-gel auto-combustion method. They concluded that the successfully produced high-purity and crystalline $MgAl_2O_4$ and $BaAl_2O_4$ spinels. The optical energy band gaps were found to be 3.676 eV for $MgAl_2O_4$ and 3.626 eV for $BaAl_2O_4$ [36]. Al-Farraj et al. prepared $MgAl_2O_4$ nanoparticles using the Pechini sol-gel method with tartaric acid as a chelating agent and propylene glycol as a cross-linker, followed by calcination at 800 °C for four hours. The resulting nanoparticles had an average crystal size of 10.36 nm and an optical band gap of 3.71 eV. They showed impressive photocatalytic performance, degrading 99.27% of congo red dye within 80 minutes at pH 3, and could be reused for four cycles. [37]. $MgAl_2O_4$ nanoparticles synthesized using Solid-state method. The synthesized nanoparticles were used to break down polyethylene plastics through photocatalytic degradation under UV light. $MgAl_2O_4$ had the narrowest energy gap 2.85 eV. and demonstrated the highest degradation rate of polyethylene 82% weight loss [38]. Liu Miao et al. Synthesised $MgAl_2O_4$ nanoparticles for the synergistic degradation of Cr(VI) ions through adsorption and photocatalysis. $MgAl_2O_4$ nanoparticles Synthesised using a sol-gel method using different chelating agents. They found that the choice of chelating agent significantly impacted the material's properties and performance in treating Cr (VI). Nanoparticles made using oxalic acid as the chelating agent showed the best adsorption and photocatalytic reduction performance, reaching 99% degradation of Cr (VI) when exposed to light.Its photocatalytic capacity was 3.56 times that of the sample made with salicylic acid [39]. Eslami Abbas and colleagues synthesized $MgAl_2O_4$ spinel nanoparticles via a sol-gel method, using stearic acid as a capping agent. The resulting nanoparticles had an average crystallite size of about 12 nm, an optical band gap of 2.84 eV, and a specific surface area of

108.1 m²/g. The nanoparticles showed ferromagnetic properties and demonstrated a remarkable hydrogen storage capacity of 4000 mAh/g [40]. Chitra Vaithiyalingam Pakkirisamy et al. synthesised $MgAl_2O_4$ nanoparticles using a hydrothermal method. The method produced cubic crystal structures of $MgAl_2O_4$. The crystallite size decreased from 22 nm to 12 nm as the reaction time increased from 6 to 24 hours, while the bandgap increased from 3.05 eV to 3.46 eV. The sample prepared over 24 hours showed the best photocatalytic activity, degrading 80% of Rhodamine B (RhB) dye in 140 minutes. It also exhibited high antibacterial activity against Staphylococcus aureus [41]. Motevalian, Arash et al. prepared $MgAl_2O_4$ nanoparticles using a sol-gel auto-ignition (combustion). The optimal fuel mixture contained 40 wt% starch, which produced pure, uniform spherical nanoparticles with a diameter of less than 13 nm and avoided significant agglomeration [42]. Ultrafine $NiAl_2O_4$ nanoparticles were synthesized using a simple one-pot chemical precipitation method. These nanoparticles featured a pure cubic phase, a crystallite size of 3.6 nm, and a band gap energy of 3.05 eV. The catalyst showed impressive efficiency in degrading malachite green (89%) and methylene blue (94%) under visible light after 120 minutes of irradiation. [43]. Patil P. et al. Developed a $NiAl_2O_4$ catalyst using a Sol-gel combustion method. The synthesized $NiAl_2O_4$ nano-catalyst was found to be highly efficient in organic synthesis. The catalyst demonstrated high yields, such as 86% for the N-phenyl formamide from aniline and formamide [44]. Xinmiao Yu and colleagues synthesized single-component $NiAl_2O_4$, ion-doped $NiAl_2O_4$, and multi-heterojunction $NiAl_2O_4$ catalysts.They have reviewed various preparation methods, including, combustion, Co-precipitation [45-47], hydrothermal [48] and sol-gel [49-51] methods. Authors have noted that the sol-gel method is ideal for producing uniform, ultrafine particles, while the sol-gel auto-combustion method combines. They found that the catalytic activity of $NiAl_2O_4$ largely depends on how it's synthesized. They also focused in the field is shifting from dye degradation to the more complex degradation of pharmaceuticals [52]. Yu Xinmiao and colleagues synthesized Nickel Aluminate ($NiAl_2O_4$) High Entropy Alloy (HEA) heterojunction photocatalysts using a polyacrylamide gel method. The resulting photocatalysts showed impressive activity in breaking down tetracycline hydrochloride (TC) under simulated sunlight. Among them, the NAO/HEA (Ti) 10% composite stood out, achieving 84.6% TC degradation in just 120 minutes. This degradation rate was significantly higher 2.97 times than that of the HEA (Ti) catalyst alone [53]. Bae Yonggyun et al. made a spinel-derived Ni catalyst on an aluminium oxide support using a powder-based solid-state reaction. The researchers have found that a uniform Ni particle of approximately 10 nm in size, which is significantly smaller than those from conventional methods. The catalyst showed the highest performance for the dry reforming of methane at low temperatures, exhibiting a lower activation energy and better stability than conventional catalysts [54]. Gayathri R. Chellammal and colleagues synthesized nickel aluminate (NA) nanoparticles using two methods sol-gel and co-precipitation at pH levels of 5, 8, and 10.5. The sol-gel method produced NA with a lower band gap (3.00 eV) compared to the co-precipitation method 3.14–3.47 eV. However, the NA synthesised by co-precipitation at pH 10.5 showed higher photocatalytic activity for degrading both tetracycline 83.26% in 30 mins and methylene blue 47.1% in 60 min. [55]. Fabricated $NiAl_2O_4$ nanostructures with different morphologies using a simple sol-gel method. The choice of capping agent determined the final morphology of the nanostructures. The $NiAl_2O_4$ nanoparticles made with glycine were used for the photocatalytic degradation of methyl orange, achieving 82% degradation after 80 minutes of UV light illumination. The material also exhibited paramagnetic behaviour at room temperature [56]. Mathubala G. Synthesised and characterised spinel $MnAl_2O_4$ nanoparticles using a facile microwave heating method. This green synthesis route used Opuntia dillenii plant extract as a reducing agent. The nanoparticles exhibited superparamagnetic properties [57]. Edrissi Mohammad et al. synthesized $MnAl_2O_4$ nanoparticles using a Pechini-modified sol–gel method. The resulting MnAl2O4 nanoparticles demonstrated good photocatalytic activity for degrading the MB solution under visible light irradiation [58]. Wang Shifa et al. $MnAl_2O_4$ nanoparticles were synthesized via the Pechini modified sol–gel method. The optimized Pechini-derived $MnAl_2O_4$ showed superior photocatalytic activity, efficiently degrading methylene blue under visible light, demonstrating strong potential for wastewater treatment applications [59]. Spinel magnesium aluminate ($MgAl_2O_4$) nanoparticles synthesized by hybrid sol-gel auto combustion method with different fuels. The $MgAl_2O_4$ synthesised with urea fuel was tested for the degradation of Reactive Red Me 4BL dye. The study found a degradation of 90.0% under UV illumination and 95.45% under sunlight irradiation within approximately 5 hours. [60]. M. Edrisi et al. successfully synthesized nanocrystalline copper aluminate ($CuAl_2O_4$) using the chelate thermolysis method. The photocatalytic performance of the synthesized $CuAl_2O_4$ was tested for breaking down crystal violet ($C_{25}N_3H_{30}Cl$) as a model pollutant, using a UV lamp as the energy source. Results showed that about 98% of the crystal violet was successfully degraded in just 120 minutes. [61]. N. Madhusudhana et al. synthesized calcium aluminate ($CaAl_2O_4$) nanoparticles were prepared by a solution combustion method. The material was used for the photocatalytic degradation of Violet GL2B azo dye under direct sunlight. The results showed that approximately 100% degradation was achieved within 120 min. [62]. Thanit Tangcharoen have synthesised the nanocrystalline alkaline earth metal spinel aluminates using a sol-gel auto combustion technique. The photocatalytic activity was tested for the degradation of four industrial dyes under natural sunlight. $MgAl_2O_4$ and $CaAl_2O_4$ showed approximately 65–89% of dye degradation within 150 minutes. The photocatalysts were reusable for up to four cycles [63]. Samvit G. Menon et al. synthesised a $CuAl_2O_4$ nanoparticles using a co-precipitation method. The material used to remove methyl orange dye from water under visible light, 67% decolouration was achieved, which increased to 100% with the addition of H_2O_2. The catalyst demonstrated excellent stability and reusability over five cycles [64]. Sattar H. Abed et al. conducted a theoretical study on $CuAl_2O_4$. This work used a computational method, Density Functional Theory (DFT), The study calculated an optical bandgap of 3.39 eV and determined that the material's electronic structure is promising for photocatalytic applications like water purification by enhancing charge transfer and reducing electron-hole recombination [65]. Chai Mei-juan et al. synthesized a mesoporous hercynite ($FeAl_2O_4$) using a simple ionic liquid self-combustion method. For the degradation of methylene blue under visible light, the material reached a yield of 47.2% in 150 minutes [66]. Cobalt aluminate ($CoAl_2O_4$) nanoparticles, synthesized using the green sol-gel method, proved effective in the photocatalytic degradation of Direct Blue 129 (DB129) and Direct Red 31 (DR31), dyes under visible light. Degradation efficiencies of 94% for DB129 and 96% for DR31 were achieved within 30 minutes. The catalyst was stable for at least four cycles [67]. Hassanzadeh-Tabrizi S. A. et al. synthesised nanostructured $CuAl_2O_4$ particles using a co-precipitation method. the formation of a single-phase spinel with a low band gap of 1.8 eV and showed the highest degradation efficiency at approximately 98% [68]. Talebi Ruhollah synthesised nanocrystalline copper aluminate ($CuAl_2O_4$) a novel and eco-friendly sol-gel method. The material's photocatalytic degradation of methyl orange under UV light evaluated. After 60 minutes of illumination, the degradation was approximately 81% [69]. Hadi Ghasemi Estarki synthesised $CuAl_2O_4$ nanoparticles using a sol-gel method. The photocatalytic efficiency, 92% degradation of methyl orange under visible light after 250 min. [70]. Myroniuk L. A. created Cu–Al–O thin films on Si substrates using the reactive ion-beam sputtering (RIBS) method. Their microstructure, morphology, optical properties, and photocatalytic activity were analyzed, and the photodegradation of $CuAl_2O_4$ films was studied using methyl orange as a model pollutant. [71]. Copper oxide (Cu_2O) and aluminium oxide (Al_2O_3) nanoparticles synthesized by facile hydrothermal method. The photodegradation of the pesticide chlorpyrifos, the nanoparticles acted as effective catalysts.100% degradation of chlorpyrifos was achieved within 31 hours [72]. Subhiksha V. et al. synthesised a $CuAl_2O_4$-Cu-$Bi_4O_5Br_2$ nanocomposite using an ultrasonication-assisted co-precipitation method. This Z-scheme heterojunction achieved over 95% degradation of both tetracycline (TET) and doxycycline (DOX) [73]. Mu et al. developed a mesoporous, earth-abundant $FeAl_2O_4$ photocatalyst using a one-step synthesis, and its photocatalytic activity was tested by degrading high concentrations of phenol [74]. Guo Mengxin et al. synthesised red mud-based biochar containing $FeAl_2O_4$ through co-pyrolysis of red mud and rice husk. The material, in conjunction with peroxydisulfate (PDS), degraded 99.5% of tetracycline in 60 minutes under visible light [75]. Naderi Mahnaz et al. synthesised nanocrystalline $CuAl_2O_4$ using the Pechini method. achieved 99% degradation of methyl orange in 110 minutes under visible light [76]. Nano-porous magnesium aluminate spinel prepared by self-combustion route method. This nano-porous magnesium aluminate spinel removed approximately 90% of the methylene blue dye in just 40 minutes under solar irradiation [77]. Wang Shifa, et al. synthesised hexagonal Barium Aluminate ($BaAl_2O_4$) catalyst using a polyacrylamide gel method. The degradation constant (k) for MB was 0.00654 min^{-1} under UV light and 0.00111 min^{-1} under simulated sunlight [78]. Faisal Shah et al. synthesised barium aluminate ($BaAl_2O_4$, BAO) and Dysprosium/Ytterbium co-doped barium aluminate using an auto combustion route method. The BAO samples exhibited fast and efficient photocatalytic activity. Pure BAO achieved over 99% degradation of MB dye in less than 40 minutes under visible light [79]. Figure (1) and (2) shows degradation of Methylene Blue and Methyl Orange using different pure aluminates photocatalysts with reaction time respectively.

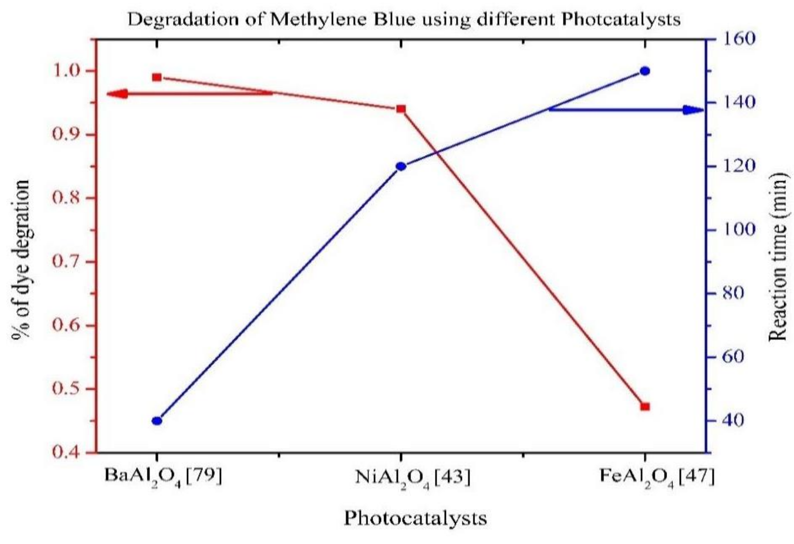

Figure 1. Dye degradation of Methylene Blue using different Photocatalysts

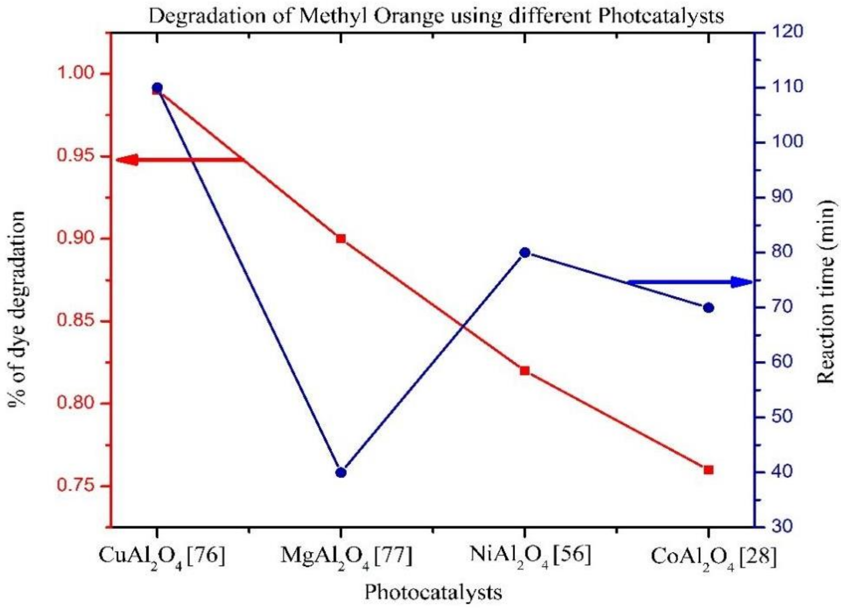

Figure 2. Dye degradation of Methyl Orang using different Photocatalysts.

It has been observed that Methylene blue 99% degraded by $BaAl_2O_4$ with reaction time less than 40 min, while Methyl Orange 99% degraded by $CuAl_2O_4$ with reaction time 110 min [79, 76].

4.2Photocatalytic Application of Doped/Mixed Spinel Aluminate:

Abd-Allah et al. synthesized zinc aluminate nanoparticles from aluminum/zinc sludge to degrade brilliant cresyl blue under visible light. They created a material with a very small bandgap energy, making it highly effective in breaking down the dye. Under optimal conditions, the photocatalytic degradation of BCBD reached 94.5% with MSS samples and 86.7% with SSR samples [80]. Elhalil A. et al. elaborated $Co_{0.5}Zn_{0.5}Al_2O_4$ spinel oxides using a co-precipitation method. the highest efficiency, achieving 98.2% degradation of methyl orange in 50 minutes under UV illumination. This high activity was attributed to a synergistic effect between adsorption and photodegradation. The catalyst was stable for up to five cycles [81]. Yu Xinmiao et al. synthesised and studied a variety of polyvalent-transition-metal-doped aluminates $(Ni_{0.2}Zn_{0.2}Mg_{0.2}Cu_{0.2}Co_{0.2})$ Al_2O_4 using a polyacrylamide gel method. This material was designed to act as a stable and efficient catalyst for degrading pollutants like levofloxacin (LEV) and tetracycline hydrochloride (TCH) by activating peroxymonosulfate (PMS). the best catalytic performance, achieving 87.0% degradation of LEV and 90.2% degradation of TCH in 90 minutes when combined with PMS under simulated sunlight [82]. Jamil Yasmin et al. investigated Cu^{2+} and Mg^{2+} doped zinc aluminate ($ZnAl_2O_4$) powders with the formula $Zn_{1-x}M_xAl_2O_4$ ($M = Cu^{2+}, Mg^{2+}$; $x = 0.10$) using a citrate-based combustion route (sol-gel method) for their structural, optical, and dielectric properties. Doping with Cu2+ and Mg2+ led to a decrease in the material's band gap and improved its dielectric properties [83]. Bhatia Sonik et al. synthesised of tin-doped ZnO (Sn-ZnO) nanoparticles with varying Sn concentrations for use as photocatalysts and gas sensors using a simple combustion method. They have concluded that the complete degradation of DR-31 dyes in 60 minutes under UV light and showed the highest sensitivity for detecting ethanol 86.80% and acetone 84.40% gas at 400 °C. [84]. K. KiranKumar et al. synthesised cerium-doped ZnAl2O4 nanoparticles using a microwave-hydrothermal method. All the samples showed a single-phase cubic spinel structure, and the lattice constant grew steadily with increased cerium doping. These characteristics make the material a good fit for ultraviolet photoelectronic devices [85]. Habibi et al. (2021) synthesized Ce-doped $ZnAl_2O_4$ particles using a simple co-precipitation chemical method. The material was an effective adsorbent for Congo red dye, with a removal efficiency of 83.88% [86]. Nasir M. et al. synthesis of zinc-doped strontium magnesium aluminium ferrite nanoparticles. The nanoparticles were prepared using a sol-gel technique. Zinc doping significantly enhanced the material's photocatalytic performance. The Zn-doped photocatalyst achieved a tetracycline degradation efficiency of 98.43%, a substantial improvement from the 73.67% efficiency of its undoped counterpart. The catalyst demonstrated excellent stability, retaining 93.45% efficiency after five cycles [87]. Chen Wei et al. synthesized a $CuAl_2O_4$/g-C_3N_4 p-n heterojunctions. They have synthesized $CuAl_2O_4$ nanoplates via a solvothermal reaction and subsequent calcination and g-C_3N_4 nanosheets were prepared by thermal polymerization. The final heterojunction was created through electrostatic self-assembly of the two components in isopropanol. The heterojunction with 10 wt% $CuAl_2O_4$ demonstrated the highest photocatalytic activity, degrading nearly 90% of TCH in one hour under visible light [88]. Barium-doped copper aluminate ($Cu_{1-x}Ba_xAl_2O_4$, where x= 0.0, 0.1, and 0.3) were synthesised using a sol-gel method by Roumaih Kh et al. (2021). Doping with Ba^{2+} ions caused a structural change from a single cubic phase to a double phase containing hexagonal $CuBaAl_{10}O_{17}$, and the morphology changed from nanograins to a mixture of nanograins and nanorods. The bandgap energy increased with Ba doping. The photocatalytic activity for methyl orange (MO) degradation was highest for the 10% Ba-doped sample 70% degradation, but the 30% doped sample showed anomalous behaviour where degradation decreased after 30 min. [89]. The thermoelectric properties of molybdenum (Mo) doped $CuAl_2O_4$ using a in-situ co-precipitation method. Mo doping successfully converted the material from p-type to n-type semiconductor and increased its carrier concentration. A device fabricated from p-type $CuAl_2O_4$ and n-type 2% Mo-doped $CuAl_2O_4$ generated an output voltage of 3.9 mV. (Chandrasekar Lakshmi Prabha et al.2024) [90]. Lin Qing et al. made zinc-doped $CuAl_2O_4$ nanofiber membranes and their application in the photocatalytic degradation of dye wastewater. An electrospinning method followed by high-temperature calcination was used. The degradation efficiency for methylene blue reached 65% after 210 minutes, an improvement of 14% over the pure $CuAl_2O_4$ membrane [91]. Ajay K. Potbhare prepared bismuth-doped copper aluminate nanocomposites using a microwave-assisted technique. The synthesized material was evaluated for biological applications. It demonstrated significant antioxidant activity, achieving a scavenging effect of 56.08% at a concentration of 500 μg/mL. It also showed effective antibacterial activity against several human pathogenic bacteria, with strong inhibition zones observed for E. coli, S. aureus, and E. faecalis [92]. Gholami Ali et al. synthesised $MgAl_2O_4$–graphene nanocomposites with graphene content varying from 1 to 5 wt%. $MgAl_2O_4$ nanoparticles were synthesised via a sol-gel method and these nanoparticles were combined with graphene in o-xylene using an ultra-sonication method. The 5% $MgAl_2O_4$–graphene nanocomposite achieved 90% degradation of methylene blue dye, compared to 70% for the pristine $MgAl_2O_4$ nanoparticles [93]. Behnamian Yashar et al. synthsised Copper aluminate-silver nanocomposite using organic acid-assisted sol-gel process. The addition of Ag significantly enhanced photocatalytic activity. The nanocomposite containing 3 wt% Ag showed the highest performance, achieving 97% degradation of methylene blue, compared to 72% for pure $CuAl_2O_4$ [94]. Arunkumar Manasai et al. synthesised Nickel-doped $CoAl_2O_4$ nanoparticles

($Co_{1-x}Ni_xAl_2O_4$, where x= 0.0 to 0.20) using a simple chemical precipitation route. The photocatalytic degradation of malachite green was effectively enhanced by nickel doping. The band gap of the nanoparticles ranged from 2.14 to 2.32 eV. The 15% Ni-doped sample ($Co_{0.85}Ni_{0.15}Al_2O_4$) demonstrated the best performance, achieving approximately 67% degradation of the dye in 120 min. [95]. Alharbi F. F. et al. developed a $CoAl_2O_4$/rGO nanohybrid to enhance the photocatalytic mineralization of methylene blue (MB). They have fabricated nanohybrid using a hydrothermal method. The $CoAl_2O_4$/rGO nanohybrid demonstrated superior photocatalytic efficiency, achieving 97.16% degradation of MB, which was significantly higher than pristine $CoAl_2O_4$ (77.51%) and rGO (88.01%) [96]. Sundararajaperumal P. et al. synthesised Neodymium (Nd^{3+}) doped $CoAl_2O_4$ nanoparticles ($Nd_x/CoAl_2O_4$, with x up to 0.6 wt%) as a photocatalyst using a sol-gel method for organic dye removal. Nd doping boosted the photocatalytic breakdown of crystal violet dye when exposed to visible light. The 0.6 wt% Nd-doped sample achieved a 91% degradation rate in 100 minutes, significantly higher than the 64% achieved by pure $CoAl_2O_4$. [97]. Boudiaf S. et al. synthesised hetero-system of $CoAl_2O_4$/ZnO. The components were prepared separately via a nitrate route, for the photo-degradation of Congo Red (CR). The hetero-system demonstrated high performance, achieving a 97% degradation of Congo Red within 4 hours under solar irradiation. Analysis of total organic carbon (TOC) confirmed a high degree of mineralization (66.9%) [98]. Irshad Amna et al. synthesised Ag-doped $NiAl_2O_4$ nanomaterials and their nanocomposites with g-C_3N_4 nanosheets to enable the photocatalytic removal of organic effluents, like methylene blue, crystal violet, and benzoic acid. A sol-gel approach was used for Ag-$NiAl_2O_4$, followed by an ultra-sonication approach for the composite. The AgNA@gCN nanocomposite demonstrated the highest photocatalytic efficiency, achieving 85.26% degradation of methylene blue, 83.87% degradation of crystal violet, and 68.46% degradation of benzoic acid under sunlight [99]. Mekkey Saleh D. et al. synthesised a series of nanostructured lanthanum-doped cobalt aluminate photocatalysts and studied their effectiveness in degrading rhodamine B (RhB) dye using a citric sol-gel method and solution-combustion synthesis. the $CoAl_{1.93}La_{0.07}O_4$ sample showing the highest efficiency, achieving 77% degradation of RhB within 250 min. [100]. Alam Mir Waqas et al. investigated chromium (Cr^{3+})-doped $MgAl_2O_4$ nanoparticles for their photocatalytic and supercapacitor applications using a solution combustion method. The Cr3+-doped $MgAl_2O_4$ showed superior performance in both applications. It achieved 89.2% degradation of Acid Red-88 dye, compared to 77.5% for the undoped material [101]. Faizan Mohd et al. synthesised Na^+ co-doped $MgAl_2O_4:Eu^{3+}$ nanostructures using a combustion method. The Na+ co-doped photocatalyst showed enhanced activity, achieving 82% degradation of Acid Navy Blue (ANB) dye in 90 minutes under visible light [102]. Jahnavi H. K. et al. synthesised a novel CaO: $MgAl_2O_4$ nanocomposite using a sol-gel method. The nanocomposite demonstrated multifunctional capabilities. For photocatalysis, it achieved 70% degradation of Acid Red-88 (AR-88) dye in 120 minutes under UV irradiation and showed significant promise in electrochemical applications, exhibiting a specific capacitance of 125 Fg^{-1} [103]. Xie et al. (2021) prepared a series of Ga-doped $MgAl_2O_4$ spinels using a homogeneous coprecipitation method. The best-performing catalyst, $MgGa_1A_{11}O_4$, reached an initial ethane conversion of 39.2% with an ethylene selectivity of 88.3%. [104]. Stojadinović Stevan et al. synthesised Eu^{3+}-doped MgAl oxide coatings containing both MgO and $MgAl_2O_4$ phases on a magnesium alloy substrate using Plasma electrolytic oxidation (PEO). The resulting coatings were composed of crystalline MgO and $MgAl_2O_4$ and exhibited the characteristic red photoluminescence of Eu^{3+} ions. The Eu^{3+}-doped coatings showed higher photocatalytic activity in degrading methyl orange than the pure MgAl oxide coating [105]. Ahmad Sajjad et al. prepared a spinel magnesium aluminate ($MgAl_2O_4$) anchored on reduced graphene oxide (rGO) nanocomposite through chemical precipitation and ultra-sonication. The composite showed improved photocatalytic performance compared to pure $MgAl_2O_4$. The band gap was reduced from 3.02 eV to 2.82 eV in the composite. Under natural sunlight, the $MgAl_2O_4$-rGO nanocomposite degraded 99.9% of Methyl Blue (MB) dye in 70 minutes and showed excellent reusability with 97% efficiency after six cycles [106]. Ali Ahmed et al. $MgAl_2O_4$–graphene nanocomposites were synthesised using an ultra-sonication method. The $MgAl_2O_4$–graphene nanocomposite containing 5% graphene showed significantly enhanced photocatalytic activity, degrading 90% of the methylene blue dye in 240 minutes under sunlight. In comparison, the pristine $MgAl_2O_4$ nanoparticles degraded only 70% [107]. Salmasi Milad Zehtab et al. Spinel $MgAl_2O_4$ nanospheres coupled with thermally-exfoliated g-C_3N_4 nanosheets (TE-GCN@$MgAl_2O_4$), using combustion and isoelectric point-assisted calcination. $MgAl_2O_4$ was prepared via combustion synthesis. The nanocomposite exhibited vastly improved photocatalytic activity. It achieved complete 100% degradation of reactive red 195 (RR195) dye in 70 minutes under simulated sunlight, significantly outperforming the individual components [108]. Manjula S. N. et al. synthesized Ho^{3+}-doped $MgAl_2O_4$ nanophosphors using a solution combustion method and investigated their photoluminescence, photocatalytic, and electrochemical sensor applications. For its photocatalytic application, it was tested for the degradation of Fast Orange-Red dye under UV light. The 9 mol% Ho^{3+}-doped sample showed the highest efficiency, achieving 89.02% decolorization in 120 min. [109]. Regulska Elzbieta et al. synthesized rare-earth metal-doped nickel aluminate spinels using the sol–gel method for the photocatalytic degradation of organic pollutants. Photocatalytic studies showed enhanced dye degradation with Mg- and Zn-doped samples: $Mg_{0.1}Ni_{0.9}Al_2O_4$ achieved 96% (MO, 90 min) and 97% (MB, 120 min), while $Zn_{0.1}Ni_{0.9}Al_2O_4$ reached 92% (MO, 180 min) and 93% (MB, 120 min), outperforming pristine $NiAl_2O_4$. [110]. $NiAl_2O_4$ (NA) and Ag-doped $NiAl_2O_4$ (AgNA) nanomaterials were synthesized via sol–gel, while their composite with g-C_3N_4 (AgNA@gCN) was prepared by ultrasonication for photocatalytic degradation of methylene blue (MB). Under sunlight, AgNA@gCN reached 85.26% MB, 83.87% CV, and 68.46% BA degradation, with overall removal efficiencies of 99.67%, 98.54%, and 76.91%, respectively. [111]. Boukha et al. synthesised magnesia-modified nickel aluminate spinel catalysts using a two-step method of precipitation followed by wet-impregnation. The catalyst's performance was strongly correlated with its surface basicity, the Mg-doped $NiAl_2O_4$ sample, with the lowest density of strong basic sites, delivered the best catalytic performance, reaching a methane conversion of 83% and an H_2 yield of 0.92, nearly matching that of a commercial Rh catalyst. [112]. Elakkiya et al. prepared nickel aluminate and doped nickel aluminate with various divalent ions (Mg, Zn, Cu) and compared their photocatalytic activity using a sol-gel method. The magnesium-doped sample ($Mg_{0.1}Ni_{0.9}Al_2O_4$) showed the highest activity, achieving 96% degradation of methyl orange in 90 minutes and 97% degradation of methylene blue in 120 min. [113]. S. Sumathi et al. synthesised cerium-doped zinc aluminate ($ZnAl_{2-x}Ce_xO_4$) nanoparticles using a co-precipitation method. the degradation of methylene blue under UV light. Cerium doping increased photocatalytic activity,99% degradation was achieved in just 20 minutes with 10 mg of the doped catalyst, compared to 80% in 180 minutes for pure $ZnAl_2O_4$ [114]. Tangcharoen et al. synthesised iron-substituted zinc aluminates ($ZnFe_xAl_{2-x}O_4$) using a sol-gel auto combustion method. The degradation of four different organic dyes under sunlight. The Fe^{3+}-substituted samples with high iron content (x = 1.5 and 2) showed superior photocatalytic activity, up to 98% degradation after 150 minutes, compared to 71% for pure $ZnAl_2O_4$ [115]. Wang Jiankang et al. synthesised a Fe_3O_4/$FeAl_2O_4$ composite coating on carbon steel using the plasma electrolytic oxidation (PEO) technique.Fenton-like system for degrading phenol. It achieved 100% removal of phenol within 60 minutes under optimal conditions and showed excellent stability [116]. Fe-doped $NiAl_2O_4$ oxides synthesised by W. Tibermacine et al. (2019) using a sol-gel method. The material was tested for its electrochemical properties, showing that $Ni_{0.7}Fe_{0.3}Al_2O_4$ had the highest catalytic activity for the oxygen evolution reaction (OER), it is approximate 27 times more active than undoped $NiAl_2O_4$ [117]. Ahmad Dilshad et al. synthesised $CuAl_2O_4$ (CAO) and N/r-GO nanohybrids.CAO was made by co-precipitation, while the nanocomposites were prepared via an ultra-sonication wet impregnation route. Under visible light, the photocatalytic removal of crystal violet dye was highly effective, with the CA-N/GO4 hybrid achieving superior performance by removing 82.6% of the dye in just 90 minutes [118]. Andrey Shelemanov et al. synthesised Cu-doped $ZnAl_2O_4$ nanocomposites using a polymer-salt method. The photocatalytic decomposition rate ($k = 0.021\ min^{-1}$) was faster than the adsorption rate, suggesting degradation occurred both on the catalyst surface and in the liquid phase [119]. Harini H. V. et al. synthesised a $Cu_2ZnAl_2O_4$ (CZA) hybrid nanostructure using a facile chemical synthesis via spontaneous combustion method. The CZA nanostructure degraded Acid Red 88 dye, achieving 91.3% degradation in 120 minutes under UV light and 63.22% under sunlight [120]. Kim Jung-Sik et al. synthesised nanocrystalline TiO_2 deposited on Ag-doped $CaAl_2O_4$: Eu^{2+}, Nd^{3+} phosphor made by conventional sintering method. The composite material showed significantly faster degradation of benzene gas under visible light compared to pure TiO_2. The Ag-doping further enhanced this activity under both UV and visible light [121]. Li Fa-tang et al. developed mixed amorphous and crystalline $MgAl_2O_4$ nano powders using a solution combustion method. The photocatalytic degradation under visible light of methylene blue, achieving 99.5% in 100 min. [122]. Myroniuk L. A. et al. synthesized Ni-doped Al_2O_3 nanoparticles using a precipitation method to study the degradation of Metanil Yellow dye under visible light. The 4 wt% Ni-doped sample achieved the highest efficiency, with 86.84% degradation after 90 minutes. [123]. Cao Mengbo et al. synthesised 3D hollow-carved Co_2 C-doped $CoAl_2O_4$ fibre composites via a simple-green pyrolysis method. It exhibited an exceptionally high maximum TC adsorption uptake of 1889.63 mg/g. Furthermore, the material could achieve 100% degradation of TC within 60 min. [124]. Zhang Jiayu et al. synthesized a range of Mg–Fe–Al–O spinels with different Mg/Al ratios through a reaction sintering process. These spinels served as heterogeneous photo-Fenton catalysts for breaking down Rhodamine B (RhB). the best performance, achieving 98.45% degradation of RhB and 83.47% Total Organic Carbon (TOC) removal [125]. Zhu Zhengru et al. prepared Ag-doped $ZnAl_2O_4$ nanorods using a hydrothermal method followed by incipient wetness impregnation. The material degraded 82% of gaseous toluene under UV light in 6 hours, outperforming undoped $ZnAl_2O_4$ [126]. Barium and bismuth Co-doped cobalt aluminate were synthesised by Zeinhom M. El-Bahy et al. using a co-precipitation route. The Ba and Bi Co-doped $CoAl_2O_4$ photocatalyst degraded 93% of benzoic acid and 92% of bromothymol blue (BTB) [127]. Abdulaziz Al-Anazi et al. synthesised mesoporous $CuAl_2O_4$/ZnO nanocomposites using an in-situ hydrothermal method. These nanocomposites were tested for their ability to degrade tetracycline (TC) under visible light.12% of $CuAl_2O_4$/ ZnO sample achieved a 100 % removal of tetracycline after 90 min. [128]. Zixi Li et al. synthesised $CoAl_2O_4/Bi_4O_5Br_2$ Z-scheme heterojunction photocatalyst through an in-situ construction method. This composite proved highly effective in breaking down tetracycline (TC) under visible light. The optimal sample achieved a 91.5% removal rate in 90 minutes [129]. Nair Anju et al. synthesised doped and co-doped nickel aluminate ($NiAl_2O_4$) using a sol-gel process with citric acid as a capping agent. The doped materials showed significantly enhanced photocatalytic activity of crystal violet dye under UV light compared to the undoped nickel aluminate. Yttrium-doped nickel aluminate achieved 97.40% degradation in 120 minutes, while the yttrium-copper co-doped version achieved 96.32% degradation in a shorter time of 90 min. [130]. Yasar M. et al. studied the photocatalytic breakdown of Congo red dye using aluminium-doped nickel cadmium manganese spinel ferrites prepared through the sol-gel auto-combustion method. The aluminum-doped catalyst showed remarkable photodegradation efficiency, removing 99.54% of Congo red dye in 60 minutes under visible light and also under optimised conditions (pH 3), 100% degradation was achieved in 30 min. [131]. Pratapkumar C. et al.

synthesised chromium (Cr^{3+}) doped magnesium aluminate nanoparticles and evaluating their photocatalytic and electrochemical properties using a self-ignited solution combustion method. The 5 mol% Cr^{3+}-doped $MgAl_2O_4$ nanoparticles showed the best performance, degrading 91.38% of Acid Red-88 dye within 150 minutes under visible light irradiation [132Alsafari Ibrahim A. created a reduced graphene oxide (r-GO) integrated nanocomposite of silver (Ag) and holmium (Ho) co-doped cobalt aluminate through a co-precipitation method followed by an ultrasonication approach. Result showed excellent photocatalytic activity for degrading rhodamine B (RhB) and benzimidazole under natural sunlight. It achieved 95.9% degradation of RhB in 150 minutes and approximately 89% degradation of benzimidazole [133]. Aljohani Meshari M. et al. synthesized a $CoAl_2O_4$/C nanocomposite as an efficient photocatalyst for degrading organic dyes using the auto-combustion method. In the photocatalytic degradation of methylene blue (MB) dye under UV light, the process achieved a 98.5% degradation efficiency within 90 minutes. [134]. Anitha G. et al. synthesized $ZnAl_2O_4$ spinel ceramics by substituting Cu^{2+}, Mg^{2+}, and Mn^{2+} at the zinc site through a sol-gel method. Among these, the Mg-doped $ZnAl_2O_4$ variants showed the fastest degradation rate, breaking down 87.5% of the organic pollutant Rose Bengal (RB) under visible light irradiation. [135]. Muneeb Muhammad et al. synthesized a $MgAl_2O_4$-Sb_2S_3 composite material using a co-precipitation method for the photocatalytic removal of Methyl Orange. Under visible light, the degradation efficiencies of a 0.1 g catalyst for MO concentrations of 1, 5, 19, 25, and 50 mg/L were 97%, 93%, 75%, 72%, and 62%, respectively. [136]. Cen Feng et al. Cr-doped $ZnAl_2O_4$ spinel photocatalyst was prepared by hydrothermal method. The highest percentage of degradation of tetracycline hydrochloride catalysed by $Zn_{0.4}Cr_{0.6}Al_2O_4$ samples at 180 min under xenon lamp irradiation was 96.02%, and the degradation percentage was increased to 97.95% at pH 3. The degradation percentage could still maintain above 90% after 5 cycles [137]. Fahoul Youssef et al. synthesised a novel $ZnAl_2O_4$/CuS nanocomposite micro-flakes using a sol-gel and a hydrothermal method. The $ZnAl_2O_4$/CuS nanocomposite achieved 95% degradation of AR1 dye within 150 min. [138]. Srinatha N. et al. synthesised a Samarium-doped zinc aluminate (Sm^{3+}-doped $ZnAl_2O_4$) nano-catalysts, using a Solution combustion method. with 3 mol% Sm^{3+} doping exhibited a remarkable degradation efficiency of 92% against AO8 dye in 120 min. [139]. Nickel-substituted cobalt aluminate spinels ($Co_{1-x}Ni_xAl_2O_4$, where x = 0.0 to 0.75) synthesised using a Co-precipitation citrate precursor technique. The composition $Co_{0.25}Ni_{0.75}Al_2O_4$ gave the highest yield of 51.93%, a significant improvement over the 30% yield obtained without a catalyst and the 45.91% yield with pure $CoAl_2O_4$.(Vaz Teotone et al.2021) [140]. Moradi Seyed Ali Hosseini et al. synthesised Erbium-doped nickel aluminate, manganese and graphene oxide (Er-doped $NiAl_2O_4$/Mn/GO) nanocomposites material using "green" synthesis approach using rhubarb extract and ultrasound-assisted method. The catalyst synthesized via the ultrasound-assisted method showed excellent photocatalytic efficiency, achieving a 94.59% degradation of Acid Black 1 dye in 60 min. [141]. Jianhui Yan et al. synthesised ZnO/CuO/$ZnAl_2O_4$ composite hollow microspheres using a polyethylene glycol (PEG)-assisted one-pot hydrothermal method. They have achieved a maximum photocatalytic degradation rate of 92.4% for MO within 60 min. [142]. Turan Büsra et al. synthesised Europium-doped Strontium Aluminate (Eu-$SrAl_2O_4$) composites using a volume combustion synthesis (VCS) method. The maximum monolayer adsorption capacities were 26.24 mg g^{-1} for tetracycline and 7.10 mg g^{-1} for ciprofloxacin. The highest adsorption occurred at pH 7, reaching 98% for tetracycline, and at pH 10, reaching 80% for ciprofloxacin [143]. Wang Shifa et al. synthesised strontium aluminate-based photocatalysts as well as Cerium (Ce) and Cerium-Manganese (Ce,Mn) co-doped $SrAl_2O_4$ for the degradation of Congo red (CR) dye using a polyacrylamide gel method. The $SrAl_2O_4$:Ce:Mn phosphor showed the highest photocatalytic degradation of Congo red (CR) dye with a rate constant of 0.00511 min^{-1} [144]. Copper aluminate coupled with tungsten trioxide ($CuAl_2O_4$-coupled

WO_3, or CAO/WO_3) heterojunctions material was developed using a one-pot polymer-aided sol-gel route method by Sobahi Tariq. The optimised sample containing 4.0% CaO/WO_3 achieved complete degradation of atrazine within 40 minutes under visible light at a concentration of 1.2 g L^{-1}[145]. Filali Hichem et al. synthesised Pure $ZnAl_2O_4$ and $ZnAl_2O_4$ dual-doped with Lanthanum and Lead nanoparticles using a citrate sol-gel route method. Under UV irradiation for 120 minutes, the sample doped with 1% La^{3+} and 2.5% Pb^{2+} (S5) degraded 70% of the HCV dye. A sample of $ZnAl_2O_4$ mixed with 50% ZnO achieved 75% degradation, while pure $ZnAl_2O_4$ degraded 57% [146]. Mumanga Takawira J.et al. synthesised neodymium-doped barium aluminate using a Combustion method. the photocatalytic degradation of methylene blue (MB) dye achieving 99% removal in 180 minutes under solar radiation [147]. Boudiaf S., et al. fabricated pure and doped cadmium aluminate nanocrystals using a facile co-precipitation route method. The photocatalytic degradation efficiency of pure, Cu-doped, Ce-doped, and co-doped $CoAl_2O_4$ against bromocresol purple (BCP) was found to be 58%, 66%, 77%, and 90%, respectively.The co-doped Cu-Ce@CAO sample exhibited the highest photocatalytic efficiency, achieving 90% degradation of bromocresol purple (BCP) and 71% degradation of benzoic acid within 120 minutes [148]. Xu Hui et al. synthesized chromium-doped metal aluminates using a simple sol-gel method. $CoAl_2O_4$: Cr proved to be the most effective catalyst, especially under the combined effects of ultrasound and simulated solar irradiation. The degradation rate constant (k) was 0.05828 min^{-1} for breaking down oil and gas field wastewater. [149]. Chen Chaoli et al. synthesised the Mn co-doped MgAl2O4:Ce composite photocatalyst using the polyacrylamide gel method. The photocatalyst showed excellent performance, achieving 88.2% degradation of rhodamine B dye after 7 hours under simulated sunlight. At a pH value of 13, the degradation rate increased to 94.3%. [150]. Wang Shifa et al. Synthesised doped and co-doped $BaAl_2O_4$ composite materials using polyacrylamide gel method. 1 g/L dosage of catalyst degraded, methylene blue (MB-5 mg/L) dye achieving 79.85% removal in 4 minutes under solar radiation [151]. Table (1) summarize dye degradation of different dyes using different mixed Spinel Aluminate and their composites.

Table (1) Dye degradation of different dyes using different mixed Spinel Aluminate and their composites

Sr. No.	dyes /Pollutants	Catalyst	Degradation (%)	Time (Min.)	Reff.
1.	Methyl Orange (MO)	$Co_{0.5}Zn_{0.5}Al_2O_4$	98.2 %	50	[81]
		$Cu_{1-x}Ba_xAl_2O_4$	70%	30	[89]
		$Mg_{0.1}Ni_{0.9}Al_2O_4$	96%	90	[110]
		$Zn_{0.1}Ni_{0.9}Al_2O_4$	92%	180	
		$Mg_{0.1}Ni_{0.9}Al_2O_4$	96%	90	
		$ZnO/CuO/ZnAl_2O_4$	92.4%	60	[142]
2.	Methyl Blue (MB)	Zinc-doped $CuAl_2O_4$	65%	210	[91]
		$MgAl_2O_4$–graphene	90%	-	[93]
		Ag-doped $CuAl_2O_4$	97%	-	[94]
		$CoAl_2O_4$/rGO	97.16%	-	[96]
		Ag-doped $NiAl_2O_4$	85.26%	-	[99]
		$MgAl_2O_4$-rGO	99.9%	70	[107]
		Ag-doped $NiAl_2O_4$	97%	120	[111]
		$Mg_{0.1}Ni_{0.9}Al_2O_4$	97%	120	[113]
		$ZnAl_{2-x}Ce_xO_4$	99%	20	[114]

		Nd^{3+}-doped $BaAl_2O_4$	99%	18	[147]
		$Ba_{1-X}B_XAl_2O_4$	79.85%	4	[151]
		Zinc-doped $CuAl_2O_4$	65%	210	[91]
3.	Tetracycline (TC)	$ZnSrMgAl_2O_4$	98.43%	-	[87]
		Doped $CoAl_2O_4$	100%	60	[124]
		$CuAl_2O_4$/ZnO (12%)	100%	120	[128]
		$Zn_{0.4}Cr_{0.6}Al_2O_4$	96.02%	180	[137]

5. Conclusion

In summary, the several types of pristine, doped spinel aluminates and their composites, their synthesis method and their efficiency of degradation of different dyes have been discussed. A wide range of metal aluminate spinel nanomaterials (MAl_2O_4 where M = Mg, Zn, Co, Ni, Cu, Ba, Sr, etc.) and their doped or composite forms have been successfully synthesized using various chemical routes—sol–gel, co-precipitation, sol-gel auto combustion, hydrothermal, electrospinning, and microwave-assisted methods. Recent advancements in synthesis techniques such as sol–gel, sol–gel auto-combustion and co-precipitation have significantly improved their efficiency, achieving more than 95% dye degradation in wastewater treatment. The sol–gel auto-combustion method is the most efficient approach for synthesizing nano-crystalline, single phase-pure spinel aluminates intended for applications in photocatalysis, antibacterial activity, or adsorption. Pristine and doped spinel aluminate oxides demonstrate strong potential as catalysts for diverse dye-degradation processes, attributed to their narrow band gaps, superior magnetic characteristics, increased surface areas, and less quantity/dosage are required.

References

1. S. Parth, U. Ashish, P. Femina, S. Manan, and S. Parin, A comprehensive review on spinel based novel catalysts for visible light assisted dye degradation. Process Saf. Environ. Prot. **161,** 703-722 (2022). https://doi.org/10.1016/j.psep.2022.03.030
2. K. Sadia, T. Noor, N. Iqbal, and L. Yaqoob, Photocatalytic dye degradation from textile wastewater: a review. ACS omega **9**, no. 20, 21751-21767 (2024). https://doi.org/10.1021/acsomega.4c00887
3. Aragaw Tadele Assefa, and Fekadu Mazengiaw Bogale, Biomass-based adsorbents for removal of dyes from wastewater: a review. Front. Environ. Sci. **9,** 764958 (2021). https://doi.org/10.3389/fenvs.2021.764958
4. KumariP reeti, and Aditya Kumar, Advanced oxidation process: A remediation technique for organic and non-biodegradable pollutant. Results Surf. Interfaces. **11,** 100122 (2023). https://doi.org/10.1016/j.rsurfi.2023.100122
5. V. -S. Kirankumar, and S. Sumathi, A review on photodegradation of organic pollutants using spinel oxide. Mater. Today Chem. **18,** 100355 (2020). https://doi.org/10.1016/j.mtchem.2020.100355
6. Han Xiulin, Meijuan Sun, Xiaona Chai, Jun Li, Yanning Wu, and Wu Sun, Progress in synthesis and photocatalytic activity of MAl_2O_4 (M= Mg, Sr, Ba) based photocatalysts. Front. Mater. **9,** 845664 (2022). https://doi.org/10.3389/fmats.2022.845664

7. Srikala, D., Kaushik, S.D. & Verma, M. Overview on Spinel Oxides: Synthesis and Applications in Various Fields. *Phys. Solid State* **66**, 327–340 (2024). https://doi.org/10.1134/S1063783424601073
8. Tetiana Tatarchuk, Basma Al-Najar, Mohamed Bououdina, and Mamdouh Abdel Aal Ahmed, Catalytic and photocatalytic properties of oxide spinels. In Handbook of Eco materials, Springer, Cham. pp. 1701-1750 (2019). https://doi.org/10.1007/978-3-319-48281-1_158-1
9. Hakki Hamid Kazemi, Peyman Aspoukeh, Hadi Seyyedbagheri, Aref Ghaderi, Samir Mustafa Hamad, Shivani R. Pandya, and Mika Sillanpää, Aluminum nanopowder from aluminum wastes recycling: a key additive for high-performance ZnO/$ZnAl_2O_4$ spinels in photocatalytic wastewater treatment. J. Sol-Gel Sci. Technol. **115**, no. 3, 1256-1272 (2025). https://doi.org/10.1007/s10971-024-06618-z
10. Javed Muhammad, and Naeem Akbar, The structural investigation and photocatalytic application of sol-gel auto-combustion derived $ZnAl_2O_4$ spinel for the degradation of organic dye. Kashmir J. Sci. **2**, no. 2, 24-37 (2023). https://doi.org/10.63147/krjs.v2i2.23
11. Bessaha Hassiba, Charef Harrats, Mohamed Bouraada, and Louis Charles Deménorval, Photocatalytic efficiency of ZnAl-layered double hydroxide on degradation of a cationic dye under UV and solar radiation. Chem. Pap. **72**, no. 4, 1031-1040 (2018). https://doi.org/10.1007/s11696-017-0347-9
12. Chaudhary Archana, Akbar Mohammad, and Shaikh M. Mobin, Facile synthesis of phase pure $ZnAl_2O_4$ nanoparticles for effective photocatalytic degradation of organic dyes. Mater. Sci. Eng. A: B **227**, 136-144 (2018). http://dx.doi.org/10.1016/j.mseb.2017.10.009
13. Putra Ageng Trisna Surya Pradana, an improved method for high photocatalytic performance of $ZnAl_2O_4$ spinel derived from layered double hydroxide precursor. SN Appl. Sci. **2**, no. 5, 842 (2020). https://doi.org/10.1007/s42452-020-2682-7
14. Ávalos-Marrón E., L. A. Diaz-Torres, C. Gómez-Solís, A. Torres-Castro, R. A. Rodríguez-Rojas, and P. García-Ramírez, Facile sol-gel synthesis of $ZnAl_2O_4$ spinel nanoceramics for photocatalytic applications: H_2 production and MB dye degradation. J. Sol-Gel Sci. Technol. **113**, no. 1, 109-122 (2025). https://doi.org/10.1007/s10971-024-06575-7
15. Han Mei, Zisheng Wang, Ye Xu, Rui Wu, Shihui Jiao, Yan Chen, and Shouhua Feng, Physical properties of $MgAl_2O_4$, $CoAl_2O_4$, $NiAl_2O_4$, $CuAl_2O_4$, and $ZnAl_2O_4$ spinels synthesized by a solution combustion method. Mater. Chem. Phys. **215**, 251-258 (2018). https://doi.org/10.1016/j.matchemphys.2018.05.029
16. Battiston Suellen, Caroline Rigo, Eric da Cruz Severo, Marcio Antonio Mazutti, Raquel Cristine Kuhn, André Gündel, and Edson Luiz Foletto, Synthesis of zinc aluminate ($ZnAl_2O_4$) spinel and its application as photocatalyst. Mater. Res. **17**, 734-738 (2014). http://dx.doi.org/10.1590/S1516-14392014005000073
17. Wang, SF., Sun, GZ., Fang, LM. et al. A comparative study of ZnAl2O4 nanoparticles synthesized from different aluminum salts for use as fluorescence materials. Sci Rep 5, 12849 (2015). https://doi.org/10.1038/srep12849
18. Tangcharoen Thanit, Jiraroj T-Thienprasert, and Chanapa Kongmark, Effect of calcination temperature on structural and optical properties of MAl_2O_4 (M= Ni, Cu, Zn) aluminate spinel nanoparticles. J. Adv. Ceram. **8**, no. 3, 352-366 (2019). https://doi.org/10.1007/s40145-019-0317-5
19. Subhan Md Abdus, Pallab Chandra Saha, Anwar Hossain, Abdullah M. Asiri, M. M. Alam, Mohammad Al-Mamun, William Ghann, Photocatalytic performance, anti-bacterial activities and 3-chlorophenol sensor fabrication using $MnAl_2O_4 \cdot ZnAl_2O_4$

nanomaterials. Nanoscale Adv. **3**, no. 20, 5872-5889 (2021). https://doi.org/10.1039/d1na00627d

20. Serdechnova M., C. Blawert, S. Karpushenkov, L. Karpushenkava, T. Shulha, P. Karlova, Rastko Vasilić, Properties of $ZnO/ZnAl_2O_4$ composite PEO coatings on zinc alloy Z1. Surf. Coat. Technol. **410** (2021). https://doi.org/10.1016/j.surfcoat.2021.126948
21. Shilpa G., K. Yogendra, K. M. Mahadevan, and N. Madhusudhana, Synthesis of $ZnAl_2O_4$ nano-particles and its application for photo-catalytic decolourization of model azo dye acid red 88 in presence of natural sunlight. IOSR J. Appl. Chem. **10**, no. 7, 35-41 (2017). DOI: 10.9790/5736-1007023541
22. Salavati Niasari Masoud, Fatemeh Davar, and Masoud Farhadi, Synthesis and characterization of spinel-type $CuAl_2O_4$ nanocrystalline by modified sol–gel method. J. Sol-Gel Sci. Technol. **51**, no. 1, 48-52 (2009). DOI 10.1007/s10971-009-1940-3
23. Khalifeh Reza, Mohammad Karimi, Maryam Rajabzadeh, Ali Hafizi, and Farhad Shahriari Nogorani, Synthesis and morphology control of nano $CuAl_2O_4$ hollow spheres and their application as an efficient and sustainable catalyst for CO_2 fixation. J. CO2 Util. **41**, 101233 (2020). https://doi.org/10.1016/j.jcou.2020.101233
24. Hosseini S. Akbar, Synthesis of $CuAl_2O_4$ nanostructures with the aid of different amino acids as a fuel and its photocatalyst application. Mater. Sci. Mater. Electron **28**, no. 4, 3762-3767 (2017). DOI:10.1007/s10854-016-5985-0
25. Dabhade Ganesh, Ankita Malpure, Ashok Borhade, Yogita Shewale, Sachin Kushare, Gaurav Daware, and Yennam Rajesh, Optical $CuAl_2O_4$ used as photocatalyst for IC dye degradation. Water Pract. Technol. **19**, no. 5, 2032-2044 (2024). **doi**: 10.2166/wpt.2024.107
26. Kaci M. M., N. Nasrallah, F. Atmani, M. Kebir, R. Guernanou, A. Soukeur, and M. Trari, Enhanced photocatalytic performance of $CuAl_2O_4$ nanoparticles spinel for dye degradation under visible light. Res. Chem. Intermed. **47**, no. 9, 3785-3806 (2021). https://doi.org/10.1007/s11164-021-04496-6
27. Abed Sattar H., and Ali H. Reshak, Optimization of $CuAl_2O_4$ nanoparticles for enhanced photocatalytic degradation of organic dyes under UV and visible light. J. Fluoresc, 1-16 (2024). https://doi.org/10.1007/s10895-024-04054-4
28. Mosleh Mohammadreza, Auto-combustion preparation and characterization of $CoAl_2O_4$ nanoparticles with different morphologies and its photocatalyst application. Mater. Sci. Mater. Electron **28**, no.1, 773-777 (2017). DOI 10.1007/s10854-016-5589-8
29. Guo Sheng, Huiling Tang, Liming You, Huali Zhang, Jun Li, and Kun Zhou, Combustion synthesis of mesoporous $CoAl_2O_4$ for peroxymonosulfate activation to degrade organic pollutants. Chin. Chem. Lett **32**, no. 9, 2828-2832 (2021). https://doi.org/10.1016/j.cclet.2021.01.019
30. Chang Ying, Ting Feng, Chonggang Wu, Yuan Chen, Kai Ke, Yang Liu, Huihu Wang, and Shijie Dong, Controlled synthesis of blue spherical $CoAl_2O_4$ pigment powder in Pickering emulsion assisted with a hydrothermal process. Adv Powder Technol. **29**, no.5, 1222-1229 (2018). https://doi.org/10.1016/j.apt.2018.02.014
31. Gholami Tahereh, Masoud Salavati-Niasari, and Shokufeh Varshoy, Investigation of the electrochemical hydrogen storage and photocatalytic properties of $CoAl_2O_4$ pigment: Green synthesis and characterization. Int. J. Hydrog. Energy **41**, no.22, 9418-9426 (2016). http://dx.doi.org/10.1016/j.ijhydene.2016.03.144
32. Devadathan Dedhila, Anju Sebastian, and B. Vidhya, Photocatalytic study of cobalt aluminate nano-particles synthesised by solution combustion method. Mater Today: Proceedings (2023). https://doi.org/10.1016/j.matpr.2023.05.641

33. Yu Fangli, Jianfeng Yang, Jingyun Ma, Jun Du, and Yongqiang Zhou, Preparation of nanosized $CoAl_2O_4$ powders by sol–gel and sol–gel-hydrothermal methods. J. Alloys Compd. **468**, no.1-2, 443-446 (2009). doi: 10.1016/j.jallcom.2008.01.018
34. Boudiaf S., N. Nasrallah, M. Mellal, C. Belabed, B. Belhamdi, D. Meziani, B. Mehdi, and M. Trari, Synthesis and characterization of semiconductor $CoAl_2O_4$ for optical and dielectric studies: application to photodegradation of organic pollutants under visible light. Optik **219**, 165038 (2020). https://doi.org/10.1016/j.ijleo.2020.165038
35. Khan Shaheer Ahmed, Zakaria Mohd Zain, Ziauddin Siddiqui, Wajahat Khan, Abdul Aabid, Muneer Baig, and Mohammad Abdul Malik, Development of Magnesium Aluminate ($MgAl_2O_4$) Nanoparticles for refractory crucible application. Plos one **19**, no.1, e0296793 (2024). https://doi.org/10.1371/journal.pone.0296793
36. Mahi, K., and Mostefa, R., Characterization of Magnesium/Barium Aluminates Spinel Synthesized by Sol-Gel Auto-Combustion Method. Vol. **14** No 2, 02025(5pp) (2022). DOI: 10.21272/jnep.14(2).02025
37. Al-Farraj, Eida S., and Ehab A. Abdelrahman, Efficient photocatalytic degradation of Congo red dye using facilely synthesized and characterized $MgAl_2O_4$ nanoparticles. ACS omega **9**, no.4, 4870-4880 (2024). https://doi.org/10.1021/acsomega.3c08485
38. Affat Sajda S., and Saad Shahad Mohammed, Photocatalytic Degradation of Polyethylene Plastics Using $MgAl_2O_4$ Nanoparticles Prepared by Solid State Method. Chem. Chem. Technol **17**, 503-509 (2023). https://doi.org/10.23939/chcht17.03.503
39. Liu Miao, Yi Wang, Yingjun Wu, Chunyang Liu, and Xin Liu, Sol-gel synthesis of magnesium aluminate and synergistic degradation of Cr (VI) ion by adsorption and photocatalysis. Front. Mater. **10**, 1274625 (2023). DOI 10.3389/fmats.2023.1274625
40. Eslami Abbas, Salahaddin Abdollah Lachini, Maryam Shaterian, Maryam Karami, and Morteza Enhessari, Sol-gel synthesis, characterization, and electrochemical evaluation of magnesium aluminate spinel nanoparticles for high-capacity hydrogen storage. J. Sol-Gel Sci. Technol. **109**, no.1, 215-225 (2024). https://doi.org/10.1007/s10971-023-06260-1
41. Chitra Vaithiyalingam Pakkirisamy, P. Vasantharani, Ganesan Sivakumar, Madhappan Santhamoorthy, Loganathan Guganathan, Sandhanasamy Devanesan, Mohamad S. Alsalhi, and Sathish Kumar Palaniappan, Preparation and characterization of $MgAl_2O_4$ nanoparticles by hydrothermal method and their photocatalytic and antibacterial activity applications. Ceram. Int. **50**, no.18, 32737-32747 (2024). https://doi.org/10.1016/j.ceramint.2024.06.083
42. Motevalian, Arash, and Shiva Salem, Effect of glycine–starch mixing ratio on the structural characteristics of $MgAl_2O_4$ nano-particles synthesized by sol–gel combustion. Particuology **24**, 108-112 (2016). http://dx.doi.org/10.1016/j.partic.2015.03.005
43. Arunkumar, M., and A. Samson Nesaraj, One pot chemical synthesis of ultrafine $NiAl_2O_4$ nanoparticles: physico-chemical properties and photocatalytic degradation of organic dyes under visible light irradiation. Inorg. Nano-Met. Chem. **51**, no. 6, 910-917 (2021). https://doi.org/10.1080/24701556.2020.1813173
44. Patil P., B. Pawar, R. Dhivare, and S. Mirgane, Nickel Aluminate (NiAl2O4): An Efficient Catalyst for Organic Transformations. Vol-**8**, 1-8 (2018).
45. N.M. Deraz, The comparative jurisprudence of catalysts preparation methods: I. precipitation and impregnation methods. J. Ind. Environ Chem. Vol-**2** (1), 19-21 (2018).
46. N. Akram, J. Guo, W. Ma, Synergistic catalysis of Co (OH) 2/CuO for the Degradation of organic pollutant under visible light irradiation, Sci Rep **10**, 1939 (2020). https://doi.org/10.1038/s41598-020-59053-9

47. X. Deng, C. Wang, H. Yang, One-pot hydrothermal synthesis of CdS decorated CuS microflower-like structures for enhanced photocatalytic properties, Sci Rep **7**, 3877 (2017). DOI:10.1038/s41598-017-04270-y
48. Z.N. Kayani, Y. Ali, F. Kiran, I. Batool, M.Z. Butt, M. Umer, S. Riaz, S. Naseem, Fabrication of copper oxide nanoparticles by sol-gel route, Mater Today: Proceedings, 2, 10, 5446-5449 (2015). doi: 10.1016/j.matpr.2015.11.067
49. Y. Vahidshad, H. Abdizadeh, H.R. Baharvandi, M. Akbari Baseri, Sol-gel synthesis and characterization of copper stabilized zirconia nanoparticles, Int. J. Mod. Phys. B **25**, (2012). DOI: 10.1142/S0217979211101119
50. Jabbar Saja Mohsen, Synthesis of CuO nano structure via sol-gel and precipitation chemical methods. Al-Khwarizmi Engineering Journal **12**, no. 4, 126-131 (2016). http://dx.doi.org/10.22153/kej.2016.07.001
51. N. Riaz, F.K. Chong, B.K. Dutta, Z.B. Man, M. Saqib Khan, E. Nurlaela, Effect of calcination temperature on Orange II photocatalytic degradation using Cu: Ni/ TiO_2 under visible light IEEE, 978-1-4577-1884-7/11 (2011). DOI: 10.1109/NatPC.2011.6136258
52. Xinmiao Yu, Shifa Wang and Huajing Gao, Spinel $NiAl_2O_4$ Based Catalysts: Past, Present and Future. J Environ Sci, 11, 12-27 (2023). https://doi.org/10.12974/2311-8741.2023.11.02
53. Yu Xinmiao, Shifa Wang, Yuanyuan Zhang, Huajing Gao, Xianju Zhou, Dengfeng Li, Hua Yang, Leiming Fang, Huijun Zhang, and Asad Syed, Novel high entropy alloy/$NiAl_2O_4$ photocatalysts for the degradation of tetracycline hydrochloride: heterojunction construction, performance evaluation and mechanistic insights. Ceram. Int. **50**, no. 17, 29528-29546 (2024). https://doi.org/10.1016/j.ceramint.2024.05.248
54. Bae Yonggyun, and Jongsup Hong, Enhancement of surface morphology and catalytic kinetics of $NiAl_2O_4$ spinel-derived Ni catalyst to promote dry reforming of methane at low temperature for the direct application to a solid oxide fuel cell. J. Chem. Eng. **446**, 136978 (2022). https://doi.org/10.1016/j.cej.2022.136978
55. Gayathri R. Chellammal, V. Elakkiya, and S. Sumathi, Effect of method of preparation on the photocatalytic activity of $NiAl_2O_4$. Inorg. Chem. Commun. **129**, 108634 (2021). https://doi.org/10.1016/j.inoche.2021.108634
56. Rahimi-Nasrabadi Mehdi, Farhad Ahmadi and Mohammad Eghbali-Arani, Different morphologies fabrication of $NiAl_2O_4$ nanostructures with the aid of new template and its photocatalyst application. Mater. Sci. Mater. Electron.**28**, no.3, 2415-2420 (2017). https://doi.org/10.1007/s10854-016-5812-7
57. Mathubala G., A facile synthesis and characterization studies of spinel $MnAl_2O_4$ nanoparticles. Malaya Journal of Matematik, Vol. S, No. **2**, 2243-2245, (2020). https://doi.org/10.26637/MJM0S20/0577
58. Edrissi Mohammad, Meysam Soleymani, and Mahnaz Naderi, Synthesis of $MnAl_2O_4$ nano crystallites by Pechini and sequential homogenous precipitation methods: characterization, product comparison, photocatalytic effect, and Taguchi optimization. J. sol-gel sci. technol. **64**, no. 2, 485-492 (2012). https://doi.org/10.1007/s10971-012-2880-x
59. Wang Shifa, Xuefeng Wei, Huajing Gao, and Yong Wei, Effect of amorphous alumina and α-alumina on optical, color, fluorescence properties and photocatalytic activity of the $MnAl_2O_4$ spinel oxides. Optik **185**, 301-310 (2019). https://doi.org/10.1016/j.ijleo.2019.03.147
60. M.Y. Nassar, I.S. Ahmed, I. Samir, A novel synthetic route for magnesium aluminate ($MgAl_2O_4$) nanoparticles using solegel auto combustion method and their photocatalytic properties. Spectrochim Acta A Mol. Biomol. Spectrosc. **131**, 329e334 (2014). https://doi.org/10.1016/j.saa.2014.04.040

61. Edrisi Mohammad, Sanaz Tajik, and Meysam Soleymani, Synthesis of $CuAl_2O_4$ nanoparticles by mixed chelates thermolysis and homogeneous precipitation using solubility difference reactions; Taguchi optimization and photocatalytic application. Mater. Sci. Mater. Electron. **24**, no.10, 3914-3920 (2013). https://doi.org/10.1007/s10854-013-1338-4
62. N. Madhusudhana, K. Yogendra, K.M. Mahadevan, Photocatalytic degradation of violet GL2B azo dye by using Calcium Aluminate nanoparticle in presence of solar light. Res. J. Chem. Sci. **2** (5), 72-77 (2012).
63. Thanit Tangcharoen, A comparative study on photodegradation of industrial dyes using alkaline earth metal spinel photocatalysts. Eur. J. Mater. VOL.**5**, NO.1, 2560346 (2025). https://doi.org/10.1080/26889277.2025.2560346
64. Menon Samvit G., Suresh D. Kulkarni, K. S. Choudhari, and Santhosh C, Diffusion-controlled growth of $CuAl_2O_4$ nanoparticles: effect of sintering and photodegradation of methyl orange. J. Exp. Nanosci. **11**, no.15, 1227-1241 (2016). https://doi.org/10.1080/17458080.2016.1209585
65. Sattar H. Abed and Ali H. Reshak, Effects of Degradation on Photocatalytic Activity and Electronic Properties of $CuAl_2O_4$: A Density Functional Theory Study. International Journal of Novel Research in Physics Chemistry & Mathematics (IJRPCM) Vol. **11**, Issue 2, pp: 72-84 (2024). https://doi.org/10.5281/zenodo.13318659
66. Chai Mei-juan, Xiang-min Chen, Ye Zhao, Rui-hong Liu, Jun Zhao, and Fa-tang Li, Facile ionic liquid combustion synthesis and visible-light photocatalytic ability of mesoporous $FeAl_2O_4$ with high specific surface area. Chem. Lett **43**, no. 11, 1743-1745 (2014). https://doi.org/10.1246/cl.140711
67. Fardood Saeid Taghavi, Farzaneh Moradnia, Sara Ganjkhanlu, Leila Ouni, Ali Ramazani, and Mika Sillanpää, Green synthesis and characterization of spinel $CoAl_2O_4$ nanoparticles: efficient photocatalytic degradation of organic dyes. Inorg. Chem. Commun. **167**, 112719 (2024). https://doi.org/10.1016/j.inoche.2024.112719
68. Hassanzadeh-Tabrizi S. A., Reza Pournajaf, Amin Moradi-Faradonbeh, and Sayed Kayvan Sadeghinejad, Nanostructured $CuAl_2O_4$: Co-precipitation synthesis, optical and photocatalytic properties. Ceram. Int.**42**, no. 12, 14121-14125 (2016). https://doi.org/10.1016/j.ceramint.2016.06.026
69. Talebi Ruhollah, Copper aluminate nanoparticles: synthesis through an eco-friendly approach and its photocatalyst application. Mater. Sci. Mater. Electron. **27**, no. 6, 5665-5669 (2016). https://doi.org/10.1007/s10854-016-4475-8
70. Hadi Ghasemi Estarki, Simple synthesize of $CuAl_2O_4$ nanoparticles by a new morphological control method, characterization of its photocatalytic activity. Mater. Sci. Mater. Electron. **28**, no. 19, 14584-14590 (2017). https://doi.org/10.1007/s10854-017-7322-7
71. Myroniuk L. A., M. G. Dusheyko, V. A. Karpyna, D. V. Myroniuk, O. I. Bykov, O. I. Olifan, O. F. Kolomys, Structural, vibrational and photodegradation properties of $CuAl_2O_4$ films. SEMICOND PHYS QUANT **25**, no. 2, 164-172 (2022). https://doi.org/10.15407/spqeo25.02.164
72. Devi Henam Sylvia, Ashaq Hussain Sofi, Thiyam David Singh, and Mohammad Ashraf Shah, Facile hydrothermal synthesis of Cu and Al oxide nanoparticles for photodegradation of chlorpyrifos. J. Nanosci. Nanotechnol. **19**, no. 12, 7707-7713 (2019). https://doi.org/10.1166/jnn.2019.16844
73. Subhiksha V., J. P. Steffy, Asad Syed, Abdallah M. Elgorban, Islem Abid, Ling Shing Wong, and S. Sudheer Khan, Novel sandwich like interfacial engineering of Cu NPs on $CuAl_2O_4$ anchored $Bi_4O_5Br_2$ nanoflower Z-scheme nano-heterojunction for enhanced photocatalytic degradation of doxycycline and tetracycline. J TAIWAN INST CHEM E **169**, 105952 (2025). https://doi.org/10.1016/j.jtice.2025.105952

74. Mu Hui-Ying, Fa-Tang Li, Xing-Tao An, Rui-Hong Liu, Yi-Lei Li, Xin Qian, and Yong-Qi Hu, One-step synthesis, electronic structure, and photocatalytic activity of earth-abundant visible-light-driven $FeAl_2O_4$. Phys. Chem. Chem. Phys. 19, no. **14**, 9392-9401 (2017). https://doi.org/10.1039/C7CP01007A
75. Guo Mengxin, Yi Han, Hongcheng Gao, Zhibing Xu, Dejin Wang, Zheng Peng, and Haobo Hou, Red mud-based biochar activated peroxydisulfate under visible light for tetracycline removal: Synergistic effect of $FeAl_2O_4$ photocatalysis. Sep. Purif. Technol. **328**, 125078 (2024). https://doi.org/10.1016/j.seppur.2023.125078
76. Naderi Mahnaz, Armen Shamirian, and Mohammad Edrisi, Synthesis, characterization and photocatalytic properties of nanoparticles $CuAl_2O_4$ by Pechini method using Taguchi statistical design. J. Sol-gel Sci. Technol. **58**, no. 2, 557-563 (2011). https://doi.org/10.1007/s10971-011-2427-6
77. Salem Shiva, Babak Nouri, and Mohammad Ghadiri, Photoactivity of magnesium aluminate under solar irradiation for treatment of wastewater contaminated by methylene blue: Effect of self-combustion factors on spinel characteristics. SOL ENERG MATER SOL C. **218**, 110773 (2020). https://doi.org/10.1016/j.solmat.2020.110773
78. Wang Shifa, Huajing Gao, Leiming Fang, Yong Wei, Yanwu Li, and Li Lei, Synthesis and characterization of $BaAl_2O_4$ catalyst and its photocatalytic activity towards degradation of methylene blue dye. Zeitschrift für Physikalische Chemie **233**, no. 8, 1161-1181 (2019). https://doi.org/10.1515/zpch-2018-1308
79. Faisal Shah, Sofi Suhail Majid, Abdul Ahad, Feroz Ahmad Sofi, Samanway Mohanta, Mukul Gupta, Pabitra Sahu, Photocatalytic Activity of $BaAl_2O_4$ for Water Purification. Langmuir **40**, no.16, 8418-8426 (2024). https://doi.org/10.1021/acs.langmuir.3c03896
80. Abd-Allah, Asmaa A., Yasser MZ Ahmed, Said M. El-Sheikh, Ahmed O. Youssef, and Amira MM Amin, Synthesis of Zinc aluminate nanoparticles from aluminum/zinc sludge for degradation of brilliant cresyl blue under visible light irradiation. J Water Environ. Nanotechnol **7**, no.3, 288-305 (2022). https://doi.org/10.22090/jwent.2022.03.005
81. Elhalil A., W. Boumya, A. Machrouhi, R. Elmoubarki, S. Mansouri, M. Sadiq, M. Abdennouri, and N. Barka, Synthesis, characterization and efficient photocatalytic properties of spinel materials for dye degradation. Appl. Surf. Sci. Adv. **13**, 100381 (2023). https://doi.org/10.1016/j.apsadv.2023.100381
82. Yu Xinmiao, Shifa Wang, Yuanyuan Zhang, Xianlun Yu, Huajing Gao, Hua Yang, Leiming Fang, Huijun Zhang, and Asad Syed, Utilization of Stable and Efficient High-Entropy ($Ni_{0.2}Zn_{0.2}Mg_{0.2}Cu_{0.2}Co_{0.2}$) Al2O4 Catalyst with Polyvalent Transition Metals to Boost Peroxymonosulfate Activation toward Pollutant Degradation. Small **21**, no. 9, 2410819 (2025). https://doi.org/10.1002/smll.202410819
83. Jamil Yasmin, Gracie P. Jeyakumar, and Geetha Deivasigamani, Investigation of Transition Metal Ions Cu^{2+} and Mg^{2+} Doped Zinc Aluminate ($ZnAl_2O_4$) and Their Structural, Spectral, Optical, and Dielectric Study for High-Frequency Applications. J. Mater. Proceedings **14**, no.1, 2 (2023). https://doi.org/10.3390/IOCN2023-14478
84. Bhatia Sonik, Neha Verma, and R. K. Bedi, Sn-doped ZnO nanopetal networks for efficient photocatalytic degradation of dye and gas sensing applications. Applied Surface Science **407**, 495-502 (2017). https://doi.org/10.1016/j.apsusc.2017.02.205
85. Kumar K. Kiran, T. Suresh Kumar, B. Ravinder Reddy, Ch Shilpa Chakra, K. Praveena, and S. Katlakunta, Structural, morphological, spectroscopic, and electrochemical properties of Cr doped $ZnAl_2O4$. J. Sol-Gel Sci. Technol. **111**, no.3, 794-805 (2024). https://doi.org/10.1007/s10971-024-06466-x

86. Habibi Milad Kohi, Seyed Mahdi Rafiaei, Amir Alhaji, and Maryam Zare, $ZnAl_2O_4$: Ce^{3+} phosphors: Study of crystal structure, microstructure, photoluminescence properties and efficient adsorption of Congo red dye. J. Mol. Struct. **1228**, 129769 (2021). https://doi.org/10.1016/j.molstruc.2020.129769
87. Nasir M., Muhammad Yasar, Abdul Maajid Khokhar, Kinza Fatima, Muzaffar Abbas, Mahrukh Ali, Faiz Mahmood, Khalid S. Almaary, Tawaf Ali Shah, and Devendra Pratap Rao, Synergistic Effect of Zn Doping on the Structural, Optical, and Photocatalytic Properties of Sol–Gel Derived Spinel Ferrite for Tetracycline Photodegradation. Catal. Lett. **155**, no.4, 1-18 (2025). https://doi.org/10.1007/s10562-025-04978-x
88. Chen Wei, Jian Huang, Zhi-Cai He, Xiong Ji, Yun-Fei Zhang, Hua-Li Sun, Kai Wang, and Zheng-Wei Su, Accelerated photocatalytic degradation of tetracycline hydrochloride over $CuAl_2O_4$/g-C_3N_4 pn heterojunctions under visible light irradiation. Sep. Purif. Technol. **277**, 119461 (2021). https://doi.org/10.1016/j.seppur.2021.119461
89. Roumaih Kh, and Shaban I. Hussein, Effect of Ba ion on phase formation, microstructure and photocatalytic properties of the $CuAl_2O_4$ nanoparticle. Eur. J. Appl. Sci **9**, no.2, 212-233 (2021). http://dx.doi.org/10.14738/aivp.92.9963
90. Chandrasekar, Lakshmi Prabha, Pandiyarasan Veluswamy, Hiroya Ikeda, and Sivakami Mohandos, Enhancing thermoelectric performance in flexible fabric-based Mo-doped $CuAl_2O_4$: Insights into carrier type modification and electrical conductivity optimization. Ceram. Int. **50**, no.22, 48330-48342 (2024). https://doi.org/10.1016/j.ceramint.2024.09.183
91. Lin Qing, Mingnan Sheng, Yuxin He, Fanxin Xu, Xiaobei Guo, Shuang Xi, Hailuo Fu, and Xiaojuan Zhang, Facile fabrication of Zn-doped $CuAl_2O_4$ nanofiber membranes for photocatalytic degradation of dye wastewater. Appl. Phys. A **130**, no. 6, 444 (2024). https://doi.org/10.1007/s00339-024-07590-9
92. Potbhare Ajay K., Prashant B. Chauke, Shadmeen Zahra, V. Sonkusare, Rina Bagade, Mayuri Ummekar, and Ratiram Gomaji Chaudhary, Microwave-mediated fabrication of mesoporous Bi-doped $CuAl_2O_4$ nanocomposites for antioxidant and antibacterial performances. Mater. Today: Proceedings **15**, 454-463 (2019). https://doi.org/10.1016/j.matpr.2019.04.107
93. Gholami Ali, and Mahnaz Maddahfar, Synthesis and characterization of novel samarium-doped $CuAl_2O_4$ and its photocatalytic performance through the modified sol–gel method. Mater. Sci. Mater. Electron. **27**, no.4, 3341-3346 (2016). https://doi.org/10.1007/s10854-015-4163-0
94. Behnamian Yashar, Ermia Aghaie, Diana Serate, Zachary Tolentino, Hamid Niazi, and Amir Mostafaei, Synthesis, characterization, and photocatalytic activity of $CuAl_2O_4$–Ag nanocomposite for water treatment. Ceram. Int. **48**, no. 19, 27988-27994 (2022). https://doi.org/10.1016/j.ceramint.2022.06.103
95. Arunkumar Manasai, and Arputharaj Samson Nesaraj, Facile chemical fabrication of Ni doped $CoAl_2O_4$ nano-spinel photocatalysts: physico-chemical properties and photodegradation of toxic malachite green dye under visible light. Int. J. Environ. Anal. Chem. **103**, no.5, 1086-1106 (2023). https://doi.org/10.1080/03067319.2020.1867722
96. Alharbi F. F., Syeda Rabia Ejaz, Abdullah G. Al-Sehemi, Muhammad Suleman Waheed, Muhammd Noman Saeed, and Hafiz Muhammad Tahir Farid, Facile fabrication of $CoAl_2O_4$ based rGO nanohybrid as an environmental purifier for photodegradation of methylene blue. Mater. Sci. Mater. Electron. **34**, no.16, 1323 (2023). https://doi.org/10.1007/s10854-023-10702-5
97. Sundararajaperumal P., P. Velusamy, M. Mahendran, and P. Sivaprakash, Influence of Nd^{3+} ions modified $CoAl_2O_4$ nanomaterials for high efficiency dye degradation

application. Ceram. Int. **50**, no.18, 34173-34183 (2024). https://doi.org/10.1016/j.ceramint.2024.06.236

98. Boudiaf, S., N. Nasrallah, M. Mellal, B. Belhamdi, C. Belabed, M. A. Djilali, and M. Trari, Kinetic studies of Congo Red Photodegradation on the hetero-system $CoAl_2O_4$/ZnO with a stirred reactor under solar light. J. Environ. Chem. Eng. **9**, no.4, 105572 (2021). https://doi.org/10.1016/j.jece.2021.105572
99. Irshad Amna, Muhammad Shahid, Salah M. El-Bahy, Islam H. El Azab, Gaber AM Mersal, Mohamed M. Ibrahim, Philips O. Agboola, and Imran Shakir, Nickel doped $CoAl_2O_4$@CNT nanocomposite: synthesis, characterization, and evaluation of sunlight driven catalytic studies. Phys. B: Condens. Matter. **636**, 413873 (2022). https://doi.org/10.1016/j.physb.2022.413873
100. Mekkey Saleh D., Mohamed E. Sultan, Mohamed M. Elsenety, Ahmed Helal, and Badr A. Elsayed, Photocatalytic degradation of rhodamine B in the visible region using nanostructured $CoAl_{2-x}La_xO_4$ (x= 0, 0.01, 0.03, 0.07, and 0.09) series: Photocatalytic activity and DFT calculations. Inorg. Chem. Commun. **136**, 109176 (2022). https://doi.org/10.1016/j.inoche.2021.109176
101. Alam Mir Waqas, VG Dileep Kumar, C. R. Ravikumar, S. C. Prashantha, HC Ananda Murthy, and MR Anil Kumar, Chromium (III) doped polycrystalline $MgAl_2O_4$ nanoparticles for photocatalytic and supercapacitor applications. J. Phys.Chem.Solids **161**, 110491 (2022). https://doi.org/10.1016/j.jpcs.2021.110491
102. Faizan Mohd, Mohd Naseem Siddique, and Sachin Kumar, Enhanced Luminescence and Photocatalytic Activity of the Monovalent Sodium (Na^+) co-doped $MgAl_2O_4$: Eu^{3+} Nanostructures. J Pure Appl Phys. (IJPAP) **62**, no.1, 9-18 (2024). https://doi.org/10.56042/ijpap.v62i1.5932
103. Jahnavi H. K., S. Rajendra Prasad, H. P. Nagaswarupa, Ramachandra Naik, N. Basavaraju, C. R. Ravikumar, Burragoni Sravanthi Goud, and Jae Hong Kim, Exploring the diverse applications of sol–gel synthesized CaO: $MgAl_2O_4$ nanocomposite: morphological, photocatalytic, and electrochemical perspectives. Discov. Nano. **19**, no. 1, 147 (2024). https://doi.org/10.1186/s11671-024-04093-7
104. Xie Qi, Changxi Miao, Weiming Hua, Yinghong Yue, and Zi Gao, Ga-doped $MgAl_2O_4$ spinel as an efficient catalyst for ethane dehydrogenation to ethylene assisted by CO_2. Ind. Eng. Chem. Res. **60**, no.31, 11707-11714 (2021). https://doi.org/10.1021/acs.iecr.1c01641
105. Stojadinović Stevan, Nenad Radić, and Rastko Vasilić, Photoluminescent and photocatalytic properties of Eu^{3+}-doped MgAl oxide coatings formed by plasma electrolytic oxidation of AZ31 magnesium alloy. Coatings **12**, no. 12, 1830 (2022). https://doi.org/10.3390/coatings12121830
106. Ahmad Sajjad, Tousif Hussain, Riaz Ahmad, Muhammad Imranullah, Urooj Shuaib, Farrukh Ehtesham Mubarik, Amna Yasin, and Umair Yaqub Qazi, Natural sunlight-driven photocatalytic degradation of methyl blue using spinel $MgAl_2O_4$-rGO nanocomposite. Appl. Nanosci. **12**, no.11, 3647-3654 (2022). https://doi.org/10.1007/s13204-022-02562-y
107. Ali Ahmed, Iftikhar Hussain Gul, Muhammad Zarrar Khan, and Farhan Javaid, Improved photocatalytic degradation efficiency of methylene blue via $MgAl_2O_4$–graphene nanocomposite. J. Korean Ceram. Soc. **60**, no. 2, 293-300 (2023). https://doi.org/10.1007/s43207-022-00263-4
108. Salmasi Milad Zehtab, Mohammad Kazemeini, Samahe Sadjadi, and Reza Nematollahi, Spinel $MgAl_2O_4$ nanospheres coupled with modified graphitic carbon nitride nanosheets as an efficient Z-scheme photocatalyst for photodegradation of organic contaminants. Appl. Surf. Sci. **585**, 152615 (2022). https://doi.org/10.1016/j.apsusc.2022.152615

109. Manjula S. N., M. Chandrasekhar, M. R. Anil Kumar, V. Bhoomika, N. Raghavendra, M. N. Somashekar, C. R. Ravikumar, and H. Nagabhushana, Studies on photoluminescence, electrochemical sensors, and photocatalysis using Ho^{3+}-doped $MgAl_2O_4$ nanophosphors. J IRAN CHEM SOC **21**, no.5, 1245-1257 (2024). https://doi.org/10.1007/s13738-024-02992-1
110. Regulska Elzbieta, Joanna Breczko, Anna Basa, and Alina Teresa Dubis, Rare-earth metals-doped nickel aluminate spinels for photocatalytic degradation of organic pollutants. Catalysts **10**, no.9, 1003 (2020). https://doi.org/10.3390/catal10091003
111. Irshad Amna, Muhammad Farooq Warsi, Philips O. Agboola, Ghulam Dastgeer, and Muhammad Shahid, Sol-gel assisted Ag doped $NiAl_2O_4$ nanomaterials and their nanocomposites with g-C_3N_4 nanosheets for the removal of organic effluents. J. Alloys Compd. **902**, 163805 (2022). https://doi.org/10.1016/j.jallcom.2022.163805
112. Boukha Zouhair, Cristina Jiménez-González, Miryam Gil-Calvo, Beatriz de Rivas, Juan Ramón González-Velasco, Jose Ignacio Gutiérrez-Ortiz, and Rubén López-Fonseca, $MgO/NiAl_2O_4$ as a new formulation of reforming catalysts: Tuning the surface properties for the enhanced partial oxidation of methane. Appl. Catal. B: Environmental **199**, 372-383 (2016). https://doi.org/10.1016/j.apcatb.2016.06.045
113. Elakkiya V., Yash Agarwal, and Shanmugam Sumathi, Photocatalytic activity of divalent ion (copper, zinc and magnesium) doped $NiAl_2O_4$. Solid State Sci. **82**, 92-98 (2018). https://doi.org/10.1016/j.solidstatesciences.2018.06.008
114. S. Sumathi, A. Kavipriya, Structural, optical and photocatalytic activity of cerium doped zinc aluminate. Solid State Sci. **65,** 52-60 (2017). https://doi.org/10.1016/j.solidstatesciences.2017.01.003
115. Tangcharoen Thanit, T. Jiraroj, and Chanapa Kongmark, Synthesis and characterization of magnetic recyclable Fe-substituted zinc aluminate photocatalysts with enhanced sunlight-driven degradation of industrial dyes. (2020). https://doi.org/10.21203/rs.3.rs-123796/v1
116. Wang Jiankang, Zhongping Yao, Min Yang, Yajing Wang, Qixing Xia, and Zhaohua Jiang, A $Fe_3O_4/FeAl_2O_4$ composite coating via plasma electrolytic oxidation on Q235 carbon steel for Fenton-like degradation of phenol. Environ. Sci. Pollut. Res. **23**, no.15, 14927-14936 (2016). https://doi.org/10.1007/s11356-016-6613-5
117. W. Tibermacine and M. Omari, Structural and electrochemical properties of Fe-doped $NiAl_2O_4$ oxides. j fundam appl sci. vol-11(1), 227-244 (2019). https://doi.org/10.4314/jfas.v11i1.
118. Ahmad Dilshad, Ismat Bibi, Farzana Majid, Shagufta Kamal, Sooman Lim, Norah Alwadai, Qasim Raza, Muhammad Aamir, Arif Nazir, and Munawar Iqbal,Impacts of r-GO and N-doping on the structural, magnetic, optical and photocatalytic properties of $CuAl_2O_4$: enhanced crystal violet removal under solar light irradiation. RSC advances **15**, no. 30, 24223-24235 (2025). DOI: 10.1039/D5RA02304A
119. Andrey Shelemanov, Artem Tincu, Sergey Evstropiev, Nikolay Nikonorov, and Vladimir Vasilyev, Cu-doped porous ZnO-$ZnAl_2O_4$ nanocomposites synthesized by polymer-salt method for photocatalytic water purification. J. Compos. Sci. **7**, no.7, 263 (2023). https://doi.org/10.3390/jcs7070263
120. Harini H. V., H. P. Nagaswarupa, Eneyew Tilahun Bekele, HC Ananda Murthy, and C. R. Ravikumar, Novel synthesis of $Cu_2ZnAl_2O_4$ nanostructures for photocatalytic and electrochemical sensor applications. Sens Int. **4** 100225 (2023). https://doi.org/10.1016/j.sintl.2022.100225
121. Kim Jung-Sik, Hyun-Je Sung, and Bum-Joon Kim, Photocatalytic characteristics for the nanocrystalline TiO2 on the Ag-doped $CaAl_2O_4$:(Eu, Nd) phosphor. Appl. Surf. Sci.**334**, 151-156 (2015). https://doi.org/10.1016/j.apsusc.2014.08.169

122. Li Fa-tang, Ye Zhao, Ying Liu, Ying-juan Hao, Rui-hong Liu, and Di-shun Zhao, Solution combustion synthesis and visible light-induced photocatalytic activity of mixed amorphous and crystalline $MgAl_2O_4$ nano powders. J. Chem. Eng. **173**, no. 3, 750-759 (2011). https://doi.org/10.1016/j.cej.2011.08.043
123. Myroniuk L. A., M. G. Dusheyko, V. A. Karpyna, D. V. Myroniuk, O. I. Bykov, O. I. Olifan, O. F. Kolomys, Structural, vibrational and photodegradation properties of CuAl2O4 films. SEMICOND PHYS QUANT **25**, no. 2, 164-172 (2022). https://doi.org/10.15407/spqeo25.02.164
124. Cao Mengbo, Xun Liu, and Hongbing Yang, Facile construction of high-performance 3D Co2C-doped CoAl2O4 fiber composites for capturing and decomposing tetracycline from aqueous solution. J. Hazard. Mater. **424**, 127307 (2022). https://doi.org/10.1016/j.jhazmat.2021.127307
125. Zhang Jiayu, Mingwei Yan, Guangchao Sun, Xiang Li, Bianlei Hao, and Kaiqi Liu, Mg–Fe–Al–O spinel: Preparation and application as a heterogeneous photo-Fenton catalyst for degrading Rhodamine B. Chemosphere **304**, 135318 (2022). https://doi.org/10.1016/j.chemosphere.2022.135318
126. Zhu Zhengru, Qidong Zhao, Xinyong Li, Hong Li, Moses Tade, and Shaomin Liu, Photocatalytic performances and activities in Ag-doped $ZnAl_2O_4$ nanorods studied by FTIR spectroscopy. Catal. Sci. Technol. **3**, no. 3, 788-796 (2013). DOI: 10.1039/C2CY20377D
127. El-Bahy Zeinhom M., Najla AlMasoud, Umaira Rafiq, Amna Irshad, Taghrid S. Alomar, Amal A. Al-Wallan, and Muhammad Farooq Warsi, Visible Light Active Ba and Bi Co-Doped $CoAl_2O_4$: Fabrication, Photocatalytic Activity against Benzoic Acid and Bromothymol Blue, and Antibacterial Studies. Phys. B: Conden. Matter. 417663 (2025). https://doi.org/10.1016/j.physb.2025.417663
128. Al-Anazi Abdulaziz, L. A. Al-Hajji, Adel A. Ismail, Ahmed Mohamed El-Toni, Aslam Khan, and Changseok Han, Visible-light-induced mesoporous ZnO hexagonal sheets decorated by $CuAl_2O_4$ nanoparticles for accelerating removal of tetracycline. Ceram. Int. **51**, no.11, 14092-14100 (2025). https://doi.org/10.1016/j.ceramint.2025.01.246
129. Zixi Li, Rui Zhang, Maoqin Xu, Jie He, Yujie Liu, Dong Chen, and Dongyuan Li, Modification of bismuth-rich to synthesize floral spherical Z-type heterojunction $CoAl_2O_4/Bi_4O_5Br_2$ photocatalysts for photocatalytic degradation of tetracycline: DFT calculations, toxicity assessment. J. Alloys Compd. **1010**, 177864 (2025). https://doi.org/10.1016/j.jallcom.2024.177864
130. Nair Anju, Ancy Kurian, Abima Samuel, and Shanmugam Sumathi, Photocatalytic degradation of crystal violet using yttrium and copper co-doped nickel aluminate. Environ. Sci. Pollut. Res. **32**, no. 7 (2025): 3746-3759. https://doi.org/10.1007/s11356-025-35913-7
131. Yasar Muhammad, Atif Mujtaba, Kinza Fatima, Maddiha Rubab, Muhammad Usman, Muhammad Jamil Khan, Devendra Pratap Rao, and Raja Waleed Sajjad, Synthesis, characterization, and photocatalytic activity of aluminum doped spinel ferrite nanoparticles for the photodegradation of Congo red. REACT KINET MECH CAT **137**, no.6, 3463-3485 (2024). https://doi.org/10.1007/s11144-024-02714-x
132. Pratapkumar C., S. C. Prashantha, VG Dileep Kumar, M. S. Santosh, C. R. Ravikumar, M. R. Anilkumar, T. S. Shashidhara, Structural, photocatalytic and electrochemical studies on facile combustion synthesized low-cost nano chromium (III) doped polycrystalline magnesium aluminate spinels. J. Sci.: Adv. Mater. Devices **6**, no.3, 462-471 (2021). https://doi.org/10.1016/j.jsamd.2021.05.009
133. Alsafari Ibrahim A., Effects of Ag/Ho-doping and reduced graphene oxide integration in cobalt aluminate spinel. Mater Chem. Phys. 131178 (2025). https://doi.org/10.1016/j.matchemphys.2025.131178

134. Aljohani Meshari M., Emad M. Masoud, Naglaa M. Mohamed, and Mostafa Y. Nassar, Cobalt aluminate/carbon nanocomposite via an auto-combustion method: an efficient photocatalyst for photocatalytic degradation of organic dyes from aqueous media. Int. J. Environ. Anal. Chem. **103**, no.19, 7979-7999 (2023). https://doi.org/10.1080/03067319.2021.1979533
135. Anitha G., G. Pavithra, and D. Geetha, Tailoring ZnAl2O4 properties through divalent metal ions (Cu^{2+}, Mg^{2+}, & Mn^{2+}) incorporation: a study on dielectric and photocatalytic enhancement. J. Mater. Sci. Mater. Electron. **36**, no.26, 1672 (2025). https://doi.org/10.1007/s10854-025-15733-8
136. Muneeb Muhammad, Bushra Ismail, Tanzeela Fazal, Abdur Rehman Khan, and Mehwish Afzia, Adsorption assisted photocatalytic removal of methyl orange by $MgAl_2O_4$-Sb_2S_3 composite material. RECENT PAT NANOTECH **10**, no.3, 213-220 (2016). https://doi.org/10.2174/1872210510666160429145814
137. Cen Feng, and Jun Li, Study on the catalytic degradation of tetracycline hydrochloride by modified spinel and its mechanism. China Surfactant Deterg. Cosmet. (2097-2806) **55**, no.4, 2097-2806 (2025). DOI: 10.3969/j.issn.2097-2806.2025.04.009
138. Fahoul Youssef, Morad Zouheir, Karim Tanji, and Abdelhak Kherbeche, Synthesis of a novel $ZnAl_2O_4$/CuS nanocomposite and its characterization for photocatalytic degradation of acid red 1 under UV illumination. J. Alloys Compd. **889**, 161708 (2021). https://doi.org/10.1016/j.jallcom.2021.161708
139. Srinatha N., S. Satyanarayana Reddy, K. Gurushantha, M. Al-Dossari, S. O. Manjunatha, and A. Madhu, Exploring the impact of Sm3+ doping on the structural, optical, and photocatalytic properties of $ZnAl_2O_4$ spinels. Ceram. Int. **50**, no.20, 37742-37753 (2024). https://doi.org/10.1016/j.ceramint.2024.07.136
140. Vaz Teotone, Pranav P. Naik, Janesline Fernandes, Lalitprabha Salgaonkar, and Snehal S. Hasolkar, Synthesis, characterization of $Co_{1-x}Ni_xAl_2O_4$ Spinel system and catalytic role in the synthesis of dihydropyrimidinone. (2021). https://doi.org/10.21203/rs.3.rs-605742/v1
141. Moradi Seyed Ali Hosseini, Durgham Abdulsattar Oleiwi, Kamran Heydaryan, Sattar H. Abed, and Farzad Namvar, UV-Responsive Er-Doped $NiAl_2O_4$/Mn/GO Nanocomposites: Green Synthesis and Photocatalytic Degradation of Organic Pollutants via Fluorescent Behaviour for Water Purification. J. Fluoresc. 1-19 (2025). https://doi.org/10.1007/s10895-025-04357-0
142. Jianhui Yan, Zhang Li, Li Xiaoyan, Zhang Xiuxiu, and Dai Chaohua, Preparation and Photocatalytic Properties of ZnO/CuO/$ZnAl_2O_4$ Composite Hollow Microspheres by One-Pot Method. Chem. Sci. Rev. Lett. 3 (2014): 12.
143. Turan Büsra, Mehmet Bugdayci, Kagan Benzesik, and Pelin Demircivi, Synthesis of Eu doped $SrAl_2O_4$ composite: adsorption characteristics on tetracycline and ciprofloxacin antibiotics. Sep. Sci. Technol. **56**, no.18, 3054-3065 (2021). https://doi.org/10.1080/01496395.2021.1878372
144. Wang Shifa, Huajing Gao, Guangzhuang Sun, Yong Wang, Leiming Fang, Liang Yang, Li Lei, and Yong Wei, Synthesis of visible-light-driven SrAl2O4-based photocatalysts using surface modification and ion doping. Russ. J. Phys. Chem. A **94**, no.6, 1234-1247 (2020). https://doi.org/10.1134/S003602442006031X
145. Sobahi Tariq, Visible-light-driven mineralization of atrazine over one-pot-synthesized $CuAl_2O_4$-coupled WO_3 heterojunction photocatalysts. Appl. Nanosci. **12**, no. 12, 4059-4068 (2022). https://doi.org/10.1007/s13204-022-02639-8
146. Filali Hichem, Nahman Boukheit, Rafika Bouhroum, Wassila Chekirou, and Ahcène Karaali, Improvement of the optical and photocatalytic properties of $ZnAl_2O_4$: 1% La^{3+}, x% Pb^{2+} nanoparticles synthesized by citrate sol-gel route. (2021). https://doi.org/10.21203/rs.3.rs-316386/v1

147. Mumanga Takawira J., Luis A. Díaz-Torres, and Christian Gómez-Solís, Nd^{3+} doped $BaAl_2O_4$ for enhanced photocatalytic degradation of methylene blue. Mater. Lett. **292**, 129664 (2021):. https://doi.org/10.1016/j.matlet.2021.129664
148. Boudiaf S., N. Nasrallah, M. Mellal, C. Belabed, B. Belhamdi, D. Meziani, B. Mehdi, and M. Trari, Synthesis and characterization of semiconductor $CoAl_2O_4$ for optical and dielectric studies: application to photodegradation of organic pollutants under visible light. Optik **219**, 165038 (2020). https://doi.org/10.1016/j.ijleo.2020.165038
149. Xu Hui, Shipeng Wang, and Rongrong Xie, Study on the Catalytic Mechanism of MAl_2O_4: Cr Catalysts (M= Mg, Co, Zn) under the Synergistic Effect of Ultrasound and Simulated Solar Irradiation on the Degradation of Oil and Gas Field Wastewater. Russ. J. Phys. Chem. A **98**, no.6, 1353-1362 (2024). https://doi.org/10.1134/S0036024424700304
150. Chen Chaoli, Qikai Li, Qing Zhang, Yanlan Li, Yong Wei, and Shifa Wang, Artificial neural network algorithm for predict the photocatalytic activity of the Mn co-doped $MgAl_2O_4$: Ce composite photocatalyst. In 2019 IEEE International Conference on Signal, Information and Data Processing (ICSIDP), pp. 1-5. IEEE (2019). DOI: 10.1109/ICSIDP47821.2019.9173359
151. Wang Shifa, Yong Wang, Huajing Gao, Jinyu Li, Leiming Fang, Xianlun Yu, Shengnan Tang, Xinxin Zhao, and Guangzhuang Sun, Synthesis and characterization of $BaAl_2O_4$: Ce and Mn-Ce-co-doped $BaAl_2O_4$ composite materials by a modified polyacrylamide gel method and prediction of photocatalytic activity using artificial neural network (ANN) algorithm. Optik **221**, 165363 (2020). https://doi.org/10.1016/j.ijleo.2020.165363